FRONTAL AND LATERAL SUBMARINE LOBE FRINGES: COMPARING SEDIMENTARY FACIES, ARCHITECTURE AND FLOW PROCESSES

YVONNE T. SPYCHALA[1†]*, DAVID M. HODGSON[1], AMANDINE PRÉLAT[2], IAN A. KANE[3] STEPHEN S. FLINT[3] and NIGEL P. MOUNTNEY[1]

[1]*Stratigraphy Group, School of Earth and Environment, University of Leeds, LS2 9JT, UK*

[2]*Beicip- Franlab, 232 Avenue Napoléon Bonaparte, 92500 Rueil-Malmaison, France*

[3]*Stratigraphy Group, School of Earth, Atmospheric and Environmental Science, University of Manchester, M13 9PL, UK*

[†]now at: Department of Earth Science, University of Utrecht, 3584 CS Utrecht, NL

**Corresponding author: Yvonne T. Spychala: y.t.spychala@uu.nl*

Keywords: basin-floor lobes, frontal fringe, lateral fringe, facies distribution, flow transformation

ABSTRACT

Submarine lobe fringe deposits form heterolithic successions that may include a high proportion of hybrid beds. The identification of lobe fringe successions aids interpretation of paleogeographic setting and the degree of basin confinement. Here, for the first time, the sedimentological and architectural differences between frontal and lateral lobe fringe deposits are investigated. Extensive outcrop and core data from Fan 4, Skoorsteenberg Formation, Karoo Basin, South Africa, allow the rates and style of facies changes from axis to fringe settings of lobes and lobe complexes in both down-dip (frontal) and across-strike (lateral) directions to be tightly constrained over an 800 km^2 study area. Fan 4 comprises three sand-prone divisions that form compensationally stacked lobe complexes, separated by thick packages of thin-bedded siltstone and sandstone intercalated with (muddy) siltstone, interpreted as the fringes of lobe complexes. Lobe-fringe facies associations comprise: i) thick-bedded structureless or planar-laminated sandstones that pinch and swell, and are associated with underlying debrites; ii) argillaceous and mudclast-rich hybrid beds; and iii) current-ripple-laminated sandstones and siltstones. Typically, frontal fringes contain high proportions of hybrid beds and transition from thick-bedded sandstones over length scales of 1 to 2 km. In contrast, lateral fringe deposits tend to comprise current ripple-laminated sandstones that transition to thick-bedded sandstones in the lobe axis over several kilometers. Variability of primary flow processes are interpreted to control the documented differences in facies association. Preferential deposition of hybrid beds in frontal fringe positions is related to the dominantly downstream momentum of the high-density core of the flow. In contrast, the ripple-laminated thin beds in lateral fringe positions are interpreted to be deposited by more dilute low-density (parts of the) flows. The development of recognition criteria to distinguish between frontal and lateral lobe fringe successions is critical to improving paleogeographic reconstructions of submarine fans at outcrop and in the subsurface, and will help to reduce uncertainty during hydrocarbon field appraisal and development.

INTRODUCTION

Traditionally, submarine lobe deposits are described as simple radial bodies that thin and fine from an apex (e.g., Mutti, 1977; Normark, 1978; Lowe, 1982; Bouma, 2000). However, it has been recognized from outcrop and geophysical studies that the anatomy of lobe deposits can be more complicated in terms of facies distribution and geometry (e.g., Nelson et al., 1992; Twichell et al., 1992; Bouma and Rozman, 2000; Gervais et al., 2006; Hodgson et al., 2006; Deptuck et al., 2008; Prélat et al., 2009; Groenenberg et al., 2010; Etienne et al., 2012). Prélat et al. (2009) proposed four sub-environments for lobe deposits that are characterized by specific facies associations and thickness trends, termed lobe axis, lobe off-axis, lobe fringe, and lobe distal fringe (Fig. 1A).

Placing constraints on the temporal and spatial variability of lobe fringe successions is important to help improve reconstructions of deep-water fans and to provide suitable building blocks for reservoir modelling and to reduce uncertainty in the evaluation of subsurface stratigraphic traps (e.g., Biddle and Wiechowsky, 1994; Etienne et al., 2012; Bakke et al., 2013; Collins et al., 2015; Grecula et al., 2015). Hybrid beds (e.g., Haughton et al., 2003; Talling et al., 2004; Haughton et al., 2009; Davis et al., 2009) and heterolithic deposits dominated by thin-bedded turbidites have been associated with lobe fringe environments (Ito, 2008; Hodgson, 2009; Talling et al., 2012a; Etienne et al., 2012; Grundvåg et al., 2014; Patacci et al., 2014; Collins et al., 2015; Fonnesu et al., 2015, Porten et al., 2016; Southern et al., 2016). Previous work on lobe fringe successions has focused on pinch-out geometries (e.g., Rozman, 2000; Marini et al., 2011; Etienne et al., 2012; Nagatomo and Archer, 2015). Some authors (e.g., MacPherson, 1978; Pickering, 1981, 1983) have documented differences between down-dip and across-strike facies transitions in lobe deposits. However, detailed depositional architecture, recognition criteria, and facies variability between down-dip (frontal) and across-strike (lateral) lobe fringe environments remain poorly constrained.

The aim of this integrated outcrop and core study is to assess the difference between frontal and lateral lobe fringe successions using the paleogeographically well-constrained Fan 4 succession of the Skoorsteenberg Formation, Karoo Basin, South Africa. Specific research objectives are as follows: 1) to establish the characteristic facies associations that distinguish the different lobe fringe settings; 2) to interpret flow processes that produce the observed facies variability; 3) to discuss the role of confinement in the distribution and character of lobe fringes; and 4) to assess the implication of the results for subsurface applications.

GEOLOGICAL SETTING

The Karoo Basin has been interpreted as a retroarc foreland basin connected to a magmatic arc and fold-thrust belt (Cape Fold Belt) (Visser and Prackelt, 1996; Visser, 1997; Catuneanu et al., 1998). Alternatively, Tankard et al. (2009) argue that subsidence during the early, deep-water, phase of deposition, which is the focus of this study, pre-dates the effects of loading by the Cape Fold Belt, and was induced by dynamic topography associated with mantle flow processes coupled to distant subduction of the paleo-Pacific plate (Pysklywec and Mitrovica, 1999). The basin fill comprises the Karoo Supergroup and records sedimentation from Late Carboniferous to Early Jurassic. The Karoo Supergroup comprises the glacial Dwyka Group, the deep-marine to shallow-marine Ecca Group and the nonmarine (fluvial) Beaufort Group. The Ecca Group, which is the focus of this study, is a shallowing-upward succession of sediments from deep-water to fluvial settings (Flint et al., 2011).

The Tanqua depocenter is located in the southwest of the Karoo Basin adjacent to the Cederberg branch of the Cape Fold Belt (Fig. 2A). Here, the Lower Ecca Group comprises the Prince Albert Formation (shallow-marine), the Whitehill Formation (deep-marine) and the Collingham Formation (deep-marine); the Upper Ecca Group comprises the Tierberg Formation (basin-plain), the Skoorsteenberg Formation (basin-floor to base-of-slope), the Kookfontein Formation (slope to shelf-edge) and the Waterford Formation (shoreface) (Fig. 2B; Bouma and Wickens, 1991; Wickens, 1994).

The Skoorsteenberg Formation (250 m thick; Bouma and Wickens, 1994) is subdivided into five sand-prone bodies. The lower four sandstone bodies (Fans 1-4) have been interpreted as basin-floor fans (Morris et al., 2000; Wickens and Bouma, 2000, Johnson et al.,2001), whereas the fifth (Unit 5) has been interpreted as a lower slope to base-of-slope system (Wickens and Bouma, 2000; Wild et al., 2005 Hodgson et al., 2006). Although a submarine fan represents a system built up by channels and lobes, the term "fan" is retained here as a lithostratigraphic descriptor for consistency with previous literature. Fans 1-4 are each up to 65 m thick, with gradational to sharp bases and tops (Johnson et al., 2001) separated by claystones and siltstones (Van der Werff and Johnson, 2003a). Each fan is interpreted as a lowstand systems tract, with the overlying fine-grained deposits of regional extent representing the related transgressive and highstand systems tracts (Goldhammer et al., 2000; Johnson et al., 2001; Hodgson et al., 2006; Hodgson, 2009).

This study focuses on the lobe deposits of Fan 4, a lobe complex-set (Fig. 1B), in an 800 km^2 study area (Fig. 2A). Fan 4 is up to 65 m thick (Johnson et al., 2001) and is characterized by a high degree of amalgamation in the Skoorsteenberg area (Fig. 3; Dudley et al., 2000). Paleocurrents and thickness distributions indicate that sediment was sourced from both the southwest and west (Dudley et al., 2000; Hodgson et al., 2006), in contrast to the underlying fans (Fans 1-3) which are point sourced from the SW. General paleocurrent orientations are to the east and northeast (Wickens and Bouma, 2000; Hodgson et al., 2006). Fan 4 is divided into two sand-rich units named the lower and upper sandstone divisions (Wickens and Bouma, 2000; Hodgson et al., 2006) separated by a thin-bedded siltstone package that is up to 6 m thick in the south and thins and fines northward. The upper division thickens to the north where the lower division thins, which was suggested by Hodgson et al. (2006) to indicate compensational stacking. The stratigraphy of Fan 4 has been revised to show that the lower sandstone division comprises one sand-prone lobe complex, whereas the upper division comprises two sand-prone lobe complexes, separated by thin-bedded heterolithic lobe-complex fringe strata.

METHODOLOGY

For this study, 24 sections were measured in strategically chosen locations (Fig. 3) in order to collect a data set that provides 3-D constraints. Graphic sedimentary logs record data on lithology, paleocurrents and bed thickness data. Detailed bed-by-bed sections (see section locations in Fig. 3; ranging from 3 to 60 m in length and totaling 510 m in cumulative thickness) record grain size, sedimentary structures and bounding surfaces of beds. Logs were recorded at 1:25 scale in the field. Four newly drilled, near-outcrop cores (see well locations on Fig. 3) intersect Fan 4 (212 m total thickness) and were logged at 1:4 scale. These data were augmented with three core logs (see locations of NOMAD –NOvel Modelled Architecture of Deepwater reservoirs – project; wells in Figure 3; 128 m cumulative thickness) and 19 graphic logs collected during previous research

(Hodgson et al., 2006; Prélat et al., 2009) (Fig. 3). Outcrop sections and core logs were redrawn at 1:50 scale for correlation purposes. The base of the mudstone and siltstone interval that separates the lower and upper sandstone division of Fan 4 was used as a correlation datum. Paleocurrent measurements (108 in total) were collected from current-ripple- and climbing-ripple-laminated sandstones, and flutes and grooves preserved as casts on bed bases. To determine facies associations and architectures of frontal and lateral fringe deposits at the scale of individual lobes, the hierarchy and paleogeography of Fan 4 was revised to improve the spatial understanding of lobe distribution.

MODEL OF LOBE ANATOMY

Hierarchy

A five-fold hierarchy of lobes in the Tanqua was proposed by Prélat et al. (2009): 1) a "bed" represents a single depositional event; 2) one or more beds form a "lobe element"; 3) several lobe elements that are divided by thin siltstone intervals stack to form a "lobe"; 4) one or more lobes stack to form a "lobe complex" (Fig. 1b). The hierarchy can be extended to the "lobe-complex set", which is formed by the stacking of one of more related lobe complexes within the same lowstand systems tract (Fig 1b). Prélat and Hodgson (2013) demonstrated that extensive meter-thick, thin-bedded units between sand-rich lobes, originally referred to as "interlobes" by Prélat et al. (2009), represent the distal fringes of lobes. Typically, these are separated from sand-rich lobe deposits (axis and off-axis) across an abrupt surface interpreted to mark an up-dip channel avulsion (Prélat and Hodgson, 2013). Thicker and more extensive thin-bedded successions can be interpreted as the fringes of lobe complexes (Prélat and Hodgson, 2013).

Sedimentary Facies and Facies Associations

Aspects of the sedimentary facies and related environments of deposition of the Skoorsteenberg Formation have been described in detail previously (e.g., Morris et al., 2000; Johnson et al., 2001; van der Werff and Johnson 2003 a, b; Hodgson et al., 2006; Luthi et al., 2006; Prélat et al., 2009; Hodgson, 2009, Jobe et al., 2012; Hofstra et al., 2015). Individual facies encountered in both outcrop (Fig. 4a-f) and core (Fig. 5a-f) datasets are summarized in Table 1. The facies combine into common facies associations representing different lobe environments: lobe axis, lobe off-axis, lobe fringe and lobe distal fringe (Prélat et al., 2009) (Fig. 1a). The boundaries between these environments are transitional. This fourfold division has been applied to several outcrop studies (e.g., Etienne et al., 2012; Prélat and Hodgson, 2013; Grundvåg et al., 2014; Spychala et al., 2015; Marchand et al., 2015; Masalimova et al., 2016). Lobe dimensions from several studies of sand-rich systems (Jegou et al., 2008; Saller et al., 2008; Deptuck et al., 2008; Prélat et al., 2009; Sømme et al., 2009) show that these bodies have elongate shapes with length-to-width ratios of 1.7 to 3.6 (Prélat et al., 2010). Average dimensions of lobes in the Tanqua depocenter are 27 km (length) × 13 km (width) × 5 m (thickness) (Fan 3, Prélat et al., 2009). Similar dimensions are expected for the lobes of Fan 4, as it was deposited under similar conditions (e.g., relatively unconfined, similar grain-size range), and similar lobe dimensions are identified across different unconfined systems (Prélat et al., 2010).

Lobe axis.---Lobe axis deposits are dominated by thick-bedded, structureless sandstone (F1; Figs. 4A, 5A; Table 1) with subordinate planar laminated (F2; Figs. 4B, 5B; Table 1) and banded sandstone (F3; Fig. 5C; Table 1) in minor proportions. The lobe axis setting is characterized as 85–100% sandstone. Multiple zones of amalgamation occur across strike (Prélat et al., 2009) and can form packages up to 5 m thick where there is scouring at the base of the lobe. The deposits of the lobe axis are laterally extensive down-dip and across strike for several hundred meters, and generally show tabular geometries (Fig. 4A). Units of high amalgamation can be traced into well-bedded units of the lobe off-axis towards the frontal and lateral margin of the lobe deposits.

Lobe off-axis.---Lobe off-axis deposits comprise well stratified medium-bedded structured sandstone (F2; Table 1) and are typically 2 to 4 m thick. Lobe off-axis deposits are characterized by 50–85% sandstone. They show tabular geometries in outcrop and can be traced out for several hundred meters in both dip and strike directions.

Lobe fringe.---Lobe fringe deposits comprise a range of facies, including structureless sandstone (F1), hybrid beds (F4; Figs. 4C,D; Table 1), debrites (F5; Fig. 5E; Table 1) and heterolithic packages (F6; Figs. 4D, 5E; Table 1). Lobe fringe deposits are characterized by 20–50% sandstone. Typical thicknesses range between 0.1 and 2 m. Several-meter-thick successions (> 2 m) are interpreted as fringes to lobe complexes; such accumulations can be walked out into thick lobate sandstone units without truncation (cf. Prélat and Hodgson, 2013). At outcrop, lobe fringe deposits can show either tapering or pinch-and-swell geometries. The pronounced pinch-and-swell geometries form lenticular bodies, even though no evidence of truncation is observed (Bouma and Rozman, 2000; Groenenberg et al., 2010). The lateral extent of lobe fringe deposits is variable and ranges from a few kilometers to several kilometers. The transition from lobe fringe to lobe distal fringe environment marks the sand pinch-out of the system.

Lobe distal fringe.---The lobe distal fringe environment is dominated by thin-bedded siltstone deposits (F7; Figs. 4e; 5g; Table 1). Some thin very fine-grained sandstone beds are intercalated in these siltstone-prone packages (< 20% sandstone). Siltstones can aggrade to form bedded successions of several meters in thickness. Lobe distal fringe deposits form an extensive "halo" around the main sand-prone lobe body and extend for several kilometers. Their dimensions have not been established.

In summary, lobe axis and off-axis deposits build the core of a lobe body and are dominated by structureless and structured sandstone. Sandstone percentage decreases towards the lobe fringe and is lowest in distal lobe fringe environments.

ARCHITECTURE

Thickness Distribution and Paleoflow Directions

Fan 4 is subdivided into a lower and upper sand-prone division, separated by a thin-bedded heterolithic division (Figs. 6, 7A). The two sand-prone divisions of Fan 4 show different thickness trends and paleocurrent patterns.

The lower, sand-prone division has a maximum thickness of ~25 m in the southern part of the study area (Fig. 6). Thinning is documented to the north and the northeast. The lower division records paleoflow to the northeast, but this trend is more northwards in the northern part of the study area (Fig. 6). Correlation panels (Fig. 7) show that down-dip pinch-out of lobe deposits occurs in several areas, such as around BK, NB2, GBE, OC7, and Ios6 area (Fig. 7). The final sand-pinch-out to the northeast occurs in the Vaalfontein-Sout Rivier area (Fig. 3). Notable lateral thinning across strike towards the east (NS3) can be observed (~5.5 m/km). Thin (< 2 m thick) siltstone deposits are deposited farther to the north, where they thin gradually.

The thin-bedded heterolithic division that separates the lower and upper sand-prone divisions of Fan 4 thins and fines over 30 km from Bizansgat in the S (~ 6 m) gradually to Sout Rivier in the N (~ 0.7 m) (Fig. 8).

The upper sand-prone division of Fan 4 has more complicated facies, thickness and paleoflow distributions. There are two areas that show high thickness values (Fig. 6). Maximum thickness in the southern study area is ~35 m (Bizansgat) from where the division thins to the north and northeast, with paleoflow trends that conform to the northeastward to northward trends of the lower division and of underlying Fan 3 (cf. Wickens and Bouma, 2000; Hodgson et al., 2006; Prélat et al., 2009). In the area around Skoorsteenberg, the upper division is 47 m thick (Fig. 6) with paleoflow trends that record a radial spread of directions from the northeast to southeast (Fig. 6; cf. Hodgson et al., 2006).

A laterally extensive ~ 3 m thick extensive thin-bedded unit is present towards the top of the upper division. Thinning also occurs to the northeast and southeast, with the rate of thinning to the northeast being highest (~ 6.9 m/km). The northeasternmost outcrops around Katjiesberg (down-dip) record dominantly northward paleocurrents and are characterized by highly variable thicknesses, which range between 2 and 14 m and reflect a pinching and swelling trend of the deposits (Fig. 6B). Correlation panels (Fig. 7) show that the oldest deposits pinch out in the Sout Rivier area, and the youngest deposits do not reach as far as the Katjiesberg area; therefore, an overall basinward to landward stacking pattern is constrained.

Hierarchy of Fan 4

Thicknesses, facies associations, and paleocurrents indicate that the lower division of Fan 4 comprises one lobe complex (Fig. 8A, LC1) that was fed by flows from the southwest. The heterolithic succession that separates the lower and upper sand-prone divisions of Fan 4 comprises thin-bedded silty mudstone, siltstone, and sandstones (heterolithic deposits) (Fig. 8B, C). The facies association, the lack of hemipelagic claystone, and the thickness patterns collectively suggest that this succession most likely represents the distal fringe of a lobe complex (cf. Prélat et al., 2009). The associated sand-prone deposits of this lobe complex (LC2) are inferred to have been located to the west, beyond the outcrop exposure. Trends in paleoflow and thickness suggest two distinct sediment entry points for the upper sand-prone division of Fan 4 (Wickens and Bouma, 2000; Dudley et al., 2000; Hodgson et al., 2006). The upper part of Fan 4 comprises two sand-prone lobe complexes (LC3 and LC5). Both of them have maximum thicknesses in the Skoorsteenberg area, and are separated by a ~ 3 m thick extensive thin-bedded unit that is interpreted as the fringe of another lobe complex (LC4; Fig. 8A).

Facies Distribution

Successive lobe deposits in weakly confined settings build lobe complexes that commonly exhibit compensational stacking patterns driven by avulsion of distributive channels (Pickering, 1981; Deptuck et al., 2008; Prélat et al., 2009; Prélat and Hodgson, 2013) (Fig. 9A-D). The distribution of sedimentary facies are described from LC1 (lower division; Fig. 10) and LC 3-5 (upper division; Fig. 10B).

In the southern part of the study area, where LC1 is thickest, the deposits are dominated by structureless (F1) and structured sandstone (F2; see Table 1; F1+F2 > 75%) (Fig. 10). The proportion of hybrid beds (F4) increases northwards where they can represent up to 50% of the thickness (e.g. Vaalfontein; Fig. 3). Heterolithic deposits (F6) dominate the basal part of LC1 around the NB2, NS2, and NS1 well locations (Fig. 3). The NS3 well is represented by heterolithic deposits (~ 70%), siltstone (~ 10%) and mudstone (~20%) (Fig. 11). Structureless sandstones are present in the northern part of the study area in highly variable proportions (15% to 50% of deposits) (Fig. 10A). Sandstone-pinch-out of the lobe complex occurs in the Sout Rivier area (Fig. 7). Northwards, the deposits of LC1 consist entirely of thin-bedded siltstones.

The upper part of Fan 4, which comprises LC3, LC4, and LC5, is characterized by a higher proportion of structureless sandstone. The southern study area is marked by structureless (F1), structured (F2), and banded sandstones (F3), which represent the bulk of deposits (50% to 75%). Hybrid beds (F4) contribute 20% of the facies composition in Koppieskraal; elsewhere they contribute less than 10%. Heterolithic deposits (F6) contribute 15% to 35% towards the central study area but less than 10% in the southern study area. The northern study area is dominated by structureless sandstone deposits (more than 50%), with the highest proportion observed in the Skoorsteenberg area (up to 80%). Structured sandstone is a minor contributor (~ 15%). Hybrid beds represent less than 10% of deposits, and heterolithic deposits commonly represent 10% to 15%. In the Katjiesberg area in the northeast, almost no heterolithic deposits are present (< 2%), but thin-siltstone deposits are intercalated with structureless sandstone and hybrid beds.

Fan 4 Paleogeographic Reconstruction

Integration of paleoflow and thickness trends with facies distribution enables reconstruction of the lower (LC1) and upper (LC3-5) divisions of the Fan 4 lobe complex set (Fig. 10). Paleoflow directions for LC1 are to both the north and the northeast (Fig. 6), whereas sediment entered from the southwest (e.g. Dudley et al., 2000; Hodgson et al., 2006). This suggests that the northward pinch-out represents a frontal fringe and the eastern termination a lateral pinch-out at the scale of the lobe complex (Fig. 7). Younger lobe deposits of LC1 pinch-out successively farther to the north, which is consistent with a progradational stacking pattern (*sensu* Hodgson et al., 2016), and frontal pinch-out at the scale of a lobe. The frontal sand pinch-out of LC1 in the Sout Rivier area (Fig. 2) is associated with a pinch-and-swell geometry of lobes and predominantly structureless sandstone and hybrid beds (Fig. 7). A "halo" of thin-bedded siltstone, which represents distal lobe fringe deposits, is deposited farther to the north. Deposits across strike (lateral) to the east are dominated by heterolithic deposits (NS3; Figs. 10, 11). The change in facies is associated with thinning of LC1. Therefore, the deposits observed in NS3 represent several lateral lobe fringes that stack to form the lobe-complex fringe. Similar facies changes have also been identified on the western margin of LC1 by Hodgson et al. (2006) in the Los Kop area (marked in Fig. 10).

The upper division of Fan 4 comprises two sand-rich lobe complexes, LC 3 and LC5, separated by an extensive thin-bedded heterolithic interval interpreted as the lobe complex fringe, LC 4. LC3 has two thick and axial zones, in the Bizansgat and in the Skoorsteensberg area (Fig. 9). The facies distribution patterns and paleoflow (Fig. 6) indicate that deposition could have been by two coeval systems with different entry points. This interpretation is supported by the lack of clear trends in facies distributions over the study area, pointing to a complicated interaction of depositional systems in the south and north. The deposits are treated as a single lobe complex because no bounding surface or extensive thin-bedded units separating the two thick and axial areas have been observed that could have been the result of avulsion. Generally, facies distributions suggest that, in the southern part of LC3, there was compensational stacking of lobes as heterolithic intervals with hybrid beds alternate with packages of structured and structureless sandstones across abrupt surfaces in vertical sections. The northern parts of LC3 and LC5 show dominantly aggradational stacking patterns of lobes (Fig. 9). Facies changes (e.g. F1 and F3) can be explained by compensational stacking on lobe-element scale (Prélat et al., 2009; Etienne et al., 2012; Prélat and Hodgson, 2013) and scouring and amalgamation of lobe axes. Abrupt facies changes from heterolithic deposits (distal lobe fringes) to sand-prone lobes suggest sufficient space for lateral compensation. In the down-dip direction (Katjiesberg) of LC3, structureless sandstone, siltstone, and hybrid beds, that show pinch-and-swell geometries, dominate the lobe complex (Fig. 13, 14). These are interpreted as stacked frontal lobe fringe deposits. The low proportion of hybrid beds otherwise in the northern part of LC3 reflects the complicated 3D geometry of individual lobes. Integration of paleocurrents and isopach maps would predict that a higher proportion of hybrid beds might be found in the subcrop to the east. Due to the complexities in LC3 and the fragmented outcrop record of LC5, the architecture of lobes, from their axes to their fringes, has focused on LC1. The results can be applied to the younger lobe complexes where data constraints permit.

LOBE FRINGE ASSOCIATIONS

Paleogeographic reconstruction of the Fan 4 lobe complex 1 (LC1) shows that lateral and frontal lobe fringe environments can be well constrained in a lobe complex using isopach maps and paleocurrents (Fig. 10). Integration of these data with mapped sand pinch-outs enables the relative position and orientation of individual lobe bodies to be determined with confidence (Fig. 10). Generally, their dip direction is to the N, whereas their strike direction is to the E and W. Figure 12 depicts characteristic transitions in facies at lateral (Fig. 12A) and frontal (Fig. 12B) lobe fringes in

LC1, which are described in detail below. Frontal and lateral lobe fringe environments are shown to display characteristic facies associations and geometries which are summarized in Table 2.

Lateral lobe fringe

Figure 12A shows a correlation panel of a single lobe from Hammerkranz to NS2 in LC1 (Figs. 3 and 10A). The lobe is defined by sharp lower and upper changes in facies to distal lobe fringe successions. Using the well-constrained paleogeographic map of LC1, this is a lateral transition from axial lobe deposits (dominated by F1 and F2) to a succession that is dominated by structured sandstone and heterolithic deposits. The lobe thins from 5.5 m in the axial position to 1.9 m in the lateral position in 4 km (0.9 m/km rate of thinning). The lower part of the lobe exhibits a transition into thin-bedded lobe fringe deposits, and the upper part of the lobe exhibits a transition to traction-dominated sandstones. Bed amalgamation is not observed.

The NS3 core (Fig. 11) shows an example of the lateral margin of a lobe complex (LC1) where all lobes pass stratigraphically into an aggradational stack of fringe deposits. The integration of observations of the detailed facies transition and the lobe fringe-dominated succession in NS3 allows the following characteristics for lateral lobe fringes to be established. The lateral lobe facies association is dominated by thin-bedded (> 0.2 m) heterolithic deposits of structureless or planar-laminated siltstone, and wavy, ripple, and climbing-ripple laminated very-fine grained sandstone (Figs. 14A, B, 15B; Table 2). Rare, debrites are present (Fig. 15B). Lateral lobe fringe deposits experience gradual decrease in sand-content (~ 50% at the transition of the lobe-off axis to ~ 20% at transition to distal lobe fringe) and bed thickness (average bed thickness of 0.6 m in lobe off axis to average bed thickness of 0.1 m in lateral lobe fringe). Therefore, pinch-out occurs over several kilometers through thinning and fining of the deposits. In outcrop (e.g. LC4; Fig. 14B), lateral lobe fringes commonly show tabular geometries at the scale of observation (Figs. 14A, B; Table 2). A similar facies transition to a lateral fringe in a lobe was well constrained in the underlying Fan 3 by Prélat et al. (2009, their Lobe 6).

Frontal Lobe Fringe

Figure 12B shows a correlation panel of a single lobe from OC2 to OC5 in LC1 (Figs. 7 and 10). The lobe is identified by abrupt lower and upper contacts to lobe distal fringe deposits. Using the well-constrained paleogeographic map of LC1, this marks the frontal transition from axial lobe deposits (dominated by F1) to a succession marked by hybrid bed deposits, structureless sandstone and siltstone beds. Sandstone deposits show a high degree of amalgamation in OC2, and become progressively less amalgamated down-dip, and increasingly intercalated with thin-bedded siltstone units (Figs. 12B and 15A). The lobe deposits exhibit a pinch-and-swell geometry (thickening from 2.5 m in OC2 to 3.2 m in OC3 and then thinning to 2 m in OC5; Fig. 12B). The sand pinch-out of the lobe occurs abruptly within few hundred meters.

Similar facies associations and geometries are observed in the frontal pinch-out of lobe deposits in termination of LC3. The frontal lobe fringe facies association is characterized by dewatered, structureless or planar-laminated fine-grained sandstones (Figs. 14C, D, 15A) associated with hybrid beds and rare thick debrites (Table 2). Commonly, the sandstone and hybrid beds of frontal lobe fringes exhibit depositional pinch-and-swell geometries (Fig. 13), which are underlain by siltstones but without any basal truncation. In map view, the pinch-and-swell geometries are mapped as irregular, finger-like bodies aligned with paleoflow (Bouma and Rozmann, 2000; Van der Werff and Johnson, 2003b; Prélat et al., 2009; Hodgson, 2009; Groenenberg et al., 2010). The dimensions of these fingers are 200-300 m in strike width and 1.5 to 2.0 km in dip length. When sand pinch-out occurs overlying sand-prone strata, pronounced fingers do not develop. The percentage of structureless sandstone within the frontal lobe fringe remains high (10 to 50%) up to the point of sandstone pinch-out. Commonly, sandstone pinch-out is abrupt, but thin-bedded siltstones typically continue for several kilometers farther.

DISCUSSION

Lobes do not show simple thinning and fining trends in all directions away from their apex (cf. Groenenberg et al., 2010). Despite showing the widest range of facies, lobe fringes are the least well studied sub-environments of lobes. Lobe fringe complexity has been highlighted by MacPherson (1978) and Pickering (1981; 1983), who demonstrated the significant variability of lobe (or fan) fringe facies. The process reasons behind the observed differences in lateral and frontal lobes fringes, and the subsurface implications of improved identification of fringe setting, are discussed below.

Controls on Lobe Pinch-Out Geometries

Generally, lateral lobe fringe successions are predominantly characterized by deposits from low-density turbidity currents, whereas frontal lobe fringes are dominated by deposits from high-density turbidity currents and other high-concentration flows (structureless sandstones, debrites, and hybrid beds; Talling et al., 2012a). Lateral lobe fringes fine and thin as they taper away from lobe axis environments (Figs. 12A, 15B). In contrast, basal lobes in the frontal fringes of lobe complexes show abrupt changes in thickness and facies (Figs. 12B, 13, 15A). Controls on this distinctive geometry in frontal lobe position could reflect either 1) influence of underlying seabed topography or 2) flow processes and interactions with substrate. Finger-like pinch-outs of frontal lobes are observed within successive lobes of multiple different lobe complexes in the Tanqua depocenter (Bouma and Rozman, 2000; Rozman, 2000; Prélat et al., 2009; Groenenberg et al., 2010). Similar terminations have been observed in other basin-floor lobe systems (Nelson et al., 1992; Twichell et al., 1992), albeit occasionally misinterpreted as channel forms (e.g. Van der Werff and Johnson, 2003b) due to their elongated shape in planform view and their convex-up form in outcrop. Groenenberg et al. (2010) did not support the presence of pre-existing seabed topography as the main influencing factor because of the common occurrence of finger-like bodies in several basal lobes over several lobe complexes. The repeated formation of seabed relief in a radial finger-like pattern prior to initiation of each lobe complexes was viewed as unlikely (Groenenberg et al., 2010).

Hybrid beds have been reported to be associated with distal lobe settings (Haughton et al., 2003; Talling et al., 2004; Ito, 2008; Hodgson, 2009; Kane and Pontén, 2012; Talling et al., 2012a; Grundvåg et al., 2014; Patacci et al., 2014; Collins et al., 2015; Fonnesu et al., 2015; Southern et al., 2016), and the cohesive nature of the depositing flows is suggested to control the abrupt pinch-out of deposits in this setting (Groenenberg et al., 2010; Kane et al., in review). In frontal lobe fringes, there is evidence that relatively distal turbidity currents eroded and entrained substrate material, preserved as mud-clasts and dispersed mud (Hodgson, 2009, Kane et al., in review). The combined effects of flow deceleration, and increased flow concentration through entrainment, led to enhanced flow stratification and the development of a dense, cohesive basal layer (e.g., McCave and Jones, 1988; Kane and Pontén, 2012; Talling, 2013; Kane et al., in review). The development of a dense basal layer in the flow may have suppressed upward transfer of turbulence, resulting in the collapse of the upper part of the flow (McCave and Jones, 1988; Kane et al., in review). The collapse of the upper part of the flow may account for the abrupt pinch-out of both the lower and upper parts of hybrid beds in distal settings, i.e., debritic divisions of hybrid beds rarely outrun the lower, cleaner sandstone division. The principal alternative, that turbidity currents fractionated their suspended load and split into forerunning turbidity currents with trailing debris flows (depositing turbidites with linked debrites; Haughton et al., 2003; Haughton et al., 2009), may account for thicker debrites, which are observed to be deposited within the finger-like structures (Fig. 13c). These may have overrun, or taken a different course, from their forerunning turbidity currents. Deposits of high-density turbidity currents are able to create their own pathways and become successively more elongated down-dip, forming finger-like bodies. These finger-like structures of frontal lobes are connected by thin beds creating a webbed bird's-foot geometry in planform (Figs. 13, 16a). This accords with results by Groenenberg et al. (2010) from process-based numerical modelling of lobes, they suggested that depositional relief of preceding lobes could help to focus these types of flow into distal areas. Elongated beds have been produced experimentally by Luthi (1981) showing that velocity of the turbidity currents was highest along the central axis. The frontal pinch-out of lobe complexes is accompanied by abrupt thickness decrease and occurs over a few hundred meters (Fig. 15A).

The lateral fringe of a lobe forms a wedge-like geometry that thins away from the lobe axis and off-axis (Fig. 15B) as deposits fine gradually over a few kilometers (Fig. 16A). Lateral lobe fringe deposits dominantly record the accumulated products of low-density turbidity currents. Luthi's (1981) experiments show that flow velocities are lowest in these flow-marginal areas, and the decrease in flow thickness is greatest laterally away from the central flow axis. Depositional relief of preceding lobe deposits probably had a relatively minor influence on low-density flows, as these can surmount seabed topography (e.g., Brunt et al., 2004; Bakke et al., 2013). Their run-out distance is therefore primarily dependent on their thickness and volume (Wynn et al., 2002). The deposits of the low-density turbidity currents probably form laterally extensive radial deposits which are higher in proportion at the lateral fringe, owing to the forward momentum and lack of lateral spreading of the higher-concentration flows in the axial areas. In the frontal fringe setting, the low-density turbidity currents, for the most-part, out ran the flows responsible for depositing the hybrid beds to deposit in distal fringe settings. Thin stand-alone debrites recorded in the lateral fringes deposits are inferred to have been deposited by debris flows which bypassed the most of the lobe to be deposited in its fringe (Talling et al., 2012b; Ducassou et al., 2013).

Role of Confinement

The difference in lateral and frontal lobe fringe in LC1 and LC3 has been documented in a relatively unconfined basin-floor setting. In basins where lobes do not feel basin confinement, compensational stacking will result in alternating successions of lobe axis and off-axis environments, with lobe fringe and distal fringe environments (Prélat and Hodgson 2013). Therefore, it is possible that frontal and lateral lobe fringes will be present in a 1-D section (e.g., core) through a single lobe complex. Flow confinement has been documented to be an important autogenic factor in the control of dispersal patterns and lobe stacking patterns (e.g. Piper and Normark, 1983; Smith and Joseph, 2004; Amy et al., 2004, Twichell et al., 2005; Macdonald et al., 2011; Marini et al., 2011; Southern et al., 2015; Marini et al., 2015).

With increased seabed confinement, lobes will be forced to stack aggradationally or longitudinally rather than compensationally. This would lead to a clearer segregation of frontal and lateral lobe fringes. Even subtle intrabasinal slopes, with angles as small as a fraction of a degree, have been shown to modify stacking patterns and facies distribution considerably. Spychala et al. (2016) show that an intrabasinal slope (< 0.5°) in the Laingsburg depocentre, Karoo Basin, led to aggradational stacking of lateral lobe fringes in multiple stacked lateral lobe-complex fringes, compared to compensational stacking patterns in the unconfined part of the basin. The aggradation of multiple lateral lobe fringes in LC1 (Fig. 11), allied to the persistent thinning and paleocurrent trends (Fig. 10) could be used to infer the presence of a subtle confining N-S oriented slope. The lateral lobe fringe facies association reflects the overall aggradational trend with sedimentary features such as climbing bedforms and predominant climbing-ripple lamination. Similar observations have been made from the Silurian sand-prone deep-water systems of the Welsh Basin (cf. Smith 1987a, 1987b; Wilson et al., 1992; Smith 2004). It is not clear if there are distinctive lateral or frontal facies trends in more highly confined basin settings; this is an area that warrants further investigation.

Subsurface Implications

The documented differences in sedimentology and architecture of lateral and frontal lobe fringes have several implications for subsurface applications. Criteria for facies recognitionestablished in this study can help determine internal division of lobe complexes in 1D datasets, e.g., core data, to help improve paleogeographic reconstructions. Stacking of lobe fringe types could be used as an indicator of the degree and orientation of seabed topography. In an unconfined setting, vertical stacking of frontal and lateral lobe fringes in a lobe complex are possible, whereas in settings influenced by relief stacked successions of frontal lobe fringes (hybrid-bed-rich deposits) or lateral lobe fringes (thin-bedded heterolithic deposits) in a lobe complex can accumulate.

Lobe fringe deposits form heterogeneities within deep-water fan deposits (e.g., Etienne et al., 2012; Collins et al., 2015; Grecula et al., 2015). Generally, frontal lobe fringes have higher sandstone percentages (~ 50%). However, the high proportion of hybrid beds means that permeability values are likely to be considerably lower than in structureless and structured sandstones. This conforms to the conclusions of Marchand et al. (2015), who observed that the presence of silt-size particles and ductile, platy-shaped grains in distal sand-rich successions decreases reservoir quality; furthermore, Porten et al. (2016) demonstrate that for a given porosity, hybrid beds may have permeabilities one or two orders of magnitude lower than turbidites. Thick-bedded deposits can be expected in frontal lobe fringes, but amalgamation is rare. Lateral fringe deposits gradually decrease in sand content (~ 50% at transition structured sandstones of the lobe-off axis to ~ 20% at transition to distal lobe fringe) and bed thickness. Bed amalgamation is not observed. Values of permeability and porosity are expected to be relatively low, and decrease gradually as the deposits thin and fine. Lobe fringes have the potential to be stratigraphic traps (*sensu* Levorsen, 1936) with their confining element being lateral depositional changes especially at the margins of a lobe complex that are encased by hemipelagic deposits. Lateral lobe fringes are dominated by lateral gradation of sandstone to silty mudstone with widespread waste zones (cf. Rittenhouse, 1972; Biddle and Wielchowsky, 1994). Frontal lobe fringes, however, are characterized by their abrupt pinch-out style (cf. Rittenhouse, 1972; Biddle and Wielchowsky, 1994) and are connected to the high-quality reservoir sandstones of the lobe axis and lobe off-axis up-dip. Therefore, frontal fringes are considered to have greater potential as viable stratigraphic trap targets.

CONCLUSIONS

Lobe fringe successions are the least well studied sub-environments of submarine lobe deposits despite showing the widest range of facies and being critical to many lobe stratigraphic-trap targets. An integrated outcrop and research borehole data set uses thickness and grain-size trends, facies distribution and depositional geometries to constrain two distinctive lobe fringe settings: frontal lobe fringe and lateral lobe fringe. Frontal lobe fringes are characterized by structureless sandstone and hybrid-bed deposits. They can exhibit elongated finger-like shapes with abrupt sandstone pinch-out. Lateral fringes are dominated by heterolithic traction-influenced deposits that gradually thin and fine to form a simple taper. Therefore, lobes do not show simple thinning and fining trends in all directions away from their apex.

The dominant flow processes control the differences in facies associations and geometries of the two lobe fringe sub-environments. Frontal lobe fringes are characterized by deposits of the highest-energy parts of turbidity currents that passed through the axis of the lobe, and maintained the highest momentum. In contrast, lateral fringes are dominated by deposits from low-density turbidity currents that are prone to tractional reworking. Distinguishing frontal and lateral lobe fringes improves prediction of facies distributions, and their stacking patterns, and can help to build more accurate reconstructions of lobe complexes, even without well-exposed outcrops arranged in 3-D distributions. Compensational stacking of lobes in unconfined settings can lead to stratigraphic alternations of frontal and lateral lobe fringes in lobe complexes, whereas it is speculated that in confined settings aggradational to longitudinal stacking of frontal and lateral fringes will result in stronger stratigraphic and geographic segregation. The development of recognition criteria to distinguish between frontal and lateral lobe fringes will help to support paleogeographic reconstructions, and inform the appraisal of stratigraphic trap prospects in the subsurface.

ACKNOWLEDGMENTS

The authors would like to thank the local farmers of the Tanqua region of South Africa for permission to carry out field studies on their land. Further, we would like to thank Aurelia Privat for field assistance. The LOBE 2 consortium project of which this research forms a part is supported by sponsorship from Anadarko, Bayerngas Norge, BG Group, BHPBilliton, BP, Chevron, DONG Energy, ENGIE, Maersk, Marathon, Petrobras, Premier Oil, Shell, Statoil, Total, VNG Norge, and Woodside, for which the authors are grateful. Reviews by the Journal of Sedimentary Research Associate Editor Morgan Sullivan and reviewers Zoltan Sylvester and Sten-Andreas Grundvåg greatly improved the manuscript.

REFERENCES

Allen, J.R.L., 1971, Instantaneous sediment deposition rates deduced from climbing-ripple cross-lamination: Geological Society of London, Journal, v. 127, p. 553-561.

Allen, J.R.L., 1973, A classification of climbing-ripple cross-lamination: Geological Society of London, Journal, v. 129, p. 537–541.

Allen, J.R.L., 1982, Sedimentary Structures: Their Character and Physical Basis vol. 1, 2: Amsterdam, Elsevier 593 p., 663 p.

Amy, L.A., McCaffrey, W.D., and Kneller, B.C., 2004, The influence of a lateral basin-slope on the depositional patterns of natural and experimental turbidity currents, *in* Joseph, P., and Lomas, S.A, eds., Deep-Water Sedimentation in the Alpine Basin of Se France: New Perspectives on the Gres d'Annot and related systems: Geological Society of London, Special Publication, 221, p. 311-330.

Arnott, R.W.C., and Hand, B.C., 1989, Bedforms, Primary structures and grain fabric in the presence of suspended sediment rain: Journal of Sedimentary Petrology, v. 59, p. 1062-1069.

Bakke, K., Kane, I.A., Martinsen, O.J., Petersen, S.A., Johansen, T.A., Hustoft, S., Jacobsen, F.H., and Groth, A., 2013, Seismic modeling in the analysis of deep-water sandstone termination style: American Association of Petroleum Geologists, Bulletin, v. 97, p. 1395- 1419.

Best, J., and Bridge, J., 1992, The morphology and dynamics of low amplitude bedwaves upon upper stage plane beds and the preservation of planar laminae: Sedimentology, *v.* 39, p. 737-752.

Biddle, K.T., and Wielchowsky, C.C., 1994, Hydrocarbon traps, *in* Magoon, L.B., and Dow, W.G., eds., The Petroleum System from Source to Trap: American Association of Petroleum Geologists, Memoir, v. 60, p. 219-235.

Bouma, A.H., 1962, Sedimentology of Some Flysch Deposits: A Graphic Approach to Facies Interpretation; Amsterdam [New York], Elsevier, , 168 p.

Bouma, A.H., and Wickens, H.d.V., 1991, Permian passive margin submarine fan complex, Karoo Basin, South Africa: possible model to Gulf of Mexico: Gulf Coast Association of Geological Societies, Transactions, v. 41, p. 30-42.

Bouma, A.H., 2000, Fine-grained, mud-rich turbidite systems: Model and comparison with coarse-grained, sand-rich systems, *in* Bouma, A.H., and Stone, C.G., eds., Fine-Grained Turbidite Systems: American Association of Petroleum Geologists, Memoir 72/SEPM, Special Publication, 68, p. 9-19.

Bouma, A.H., and Rozman, D.J., 2000, Characteristics of fine grained outer fan fringe turbidite systems, *in* Bouma, A.H., and Stone, C.G., eds., Fine-Grained Turbidite Systems: American Association of Petroleum Geologists,Memoir 72/SEPM, Special Publication,. 68, p. 291–298.

Brunt, R.L., McCaffrey, W.D., and Kneller, B.C., 2004, Experimental modeling of the spatial distribution of grain size developed in a fill-and-spill mini-basin setting: Journal of Sedimentary Research, v. 74, p. 438-446.

Catuneanu, O., Hancox, P.J., and Rubridge, B.S., 1998, Reciprocal flexural behaviour and contrasting stratigraphies: a new basin development model for the Karoo retroarc foreland system, South Africa: Basin Research, v. 10, p. 417-439.

Collins, J., Kenyon-Roberts, S., Cullen, B., White, J., Bordas-Le Floch, N., and Downey, J., 2015, Arran Field: a complex heterolithic reservoir on the margins of the Forties Fan System, *in* McKie, T., Rose, P.T.S., Hartley, A.J., Jones, D.W. and Armstrong, T.L., eds., Tertiary Deep-Marine Reservoirs of the North Sea Region: Geological Society of London, Special Publication,. 403, p. 185-217.

Davis, C., Haughton, P., McCaffrey, W., Scott, E. Hogg, N., and Kitching, D., 2009, Character and distribution of hybrid sediment gravity flow deposits from the outer Forties Fan, Paleocene Central North Sea, UKCS: Marine and Petroleum Geology, v. 26, p. 1919-1939.

Deptuck, M.E., Piper, D.J.W., Savoye, B., and Gervais, A., 2008, Dimensions and architecture of late Pleistocene submarine lobes off the northern margin of East Corsica: Sedimentology, v. 55, p. 869–898.

Ducassou, E., Migeon, S., Capotondi, L., and Mascle, J., 2013, Run-out distance and erosion of debris-flows in the Nile deep-sea fan system: Evidence from lithofacies and micropaleontological analyses: Marine and Petroleum Geology, v. 38, p. 102-123.

Dudley, P.R.C., Rehmer, D.E., and Bouma, A.H., 2000, Reservoir-scale characteristics of fine-grained sheet sandstone, Tanqua Karoo Subbasin, South Africa: Gulf Coast Section SEPM Foundation 20th Annual Research Conference, Deep-Water Reservoirs of the World, December 3-6, p. 318-314.

Etienne, S., Mulder, T., Bez, M., Desaubliaux, G., Kwasniewski, A., Parize, O., Dujoncquoy, E., and Salles, T., 2012, Multiple scale characterization of sand-rich distal lobe deposit variability: Examples from the Annot Sandstones Formation, Eocene–Oligocene, SE France: Sedimentary Geology, v. 273-274, p. 1-18.

Flint, S.S., Hodgson, D.M., Sprague, A.R., Brunt, R.L., van der Merwe, W.C., Figueiredo, J., Prélat, A., Box, D., Di Celma, C., and Kavanagh, J.P., 2011, Depositional architecture and sequence stratigraphy of the Karoo basin floor to shelf edge succession, Laingsburg depocentre, South Africa: Marine and Petroleum Geology, v. 28, p. 658-674.

Fonnesu, M., Haughton, P., Felletti, F., and McCaffrey, W., 2015, Short length-scale variability of hybrid event beds and its applied significance: Marine and Petroleum Geology, v. 67, p. 583-603.

Gervais, A., Savoye, B., Mulder, T., and Gonthier, E., 2006, Sandy modern turbidite lobes: A new insight from high resolution seismic data: Marine and Petroleum Geology, v. 23, p. 485-502.

Goldhammer, R.K., Wickens, D.H., Bouma, A.H., and Wach, G., 2000, Sequence Stratigraphic Architecture of the Late Permian Tanqua Submarine Fan Complex, Karoo Basin, South Africa, , *in*

Bouma, A.H., and Stone, C.G., eds., Fine-Grained Turbidite Systems: American Association of Petroleum Geologists, Memoir 72/SEPM, Special Publication,. 68, p. 165-172.

Grecula, M., Hognestad, J., Price, S., Boya Ferrero, M., De Brujin, G., Noraberg, K.T., Engenes, K., Mears, P., Van Ojik, K., and McGarva, R., 2015, Interplay of fan-fringe reservoir detieriation and hydrodynamic aquifer: understanding the margins of gas development in the Ormen Lange Field, *in* McKie, T., Rose, P.T.S., Hartley, A.J., Jones, D.W., and Armstrong, T.L., eds., Tertiary Deep-Marine Reservoirs of the North Sea Region: Geological Society of London, Special Publication,. 403, p.157-183.

Groenenberg, R.M., Hodgson, D.M., Prélat, A., Luthi, S.M., and Flint, S.S., 2010, Flow-deposit interaction in submarine lobes: Insights from outcrop observations and realizations of the process-based numerical model: Journal of Sedimentary Research, v. 80, p. 252-267.

Grundvåg, S.A., Johannessen, E.P., Helland-Hansen, W., and Plink-Björklund, P., 2014, Depositional architecture and evolution of progradationally stacked lobe complexes in the Eocene Central Basin of Spitsbergen: Sedimentology, v. 61, p. 535-569.

Haughton, P.D.W., Barker, S.P., and McCaffrey, W.D., 2003, 'Linked' debrites in sand-rich turbidite systems – Origin and significance: Sedimentology, v. 50, p. 459-482.

Haughton, P., Davis, C., McCaffrey, W., and Barker, S., 2009, Hybrid sediment gravity flow deposits – Classification, origin and significance: Marine and Petroleum Geology, v. 26, p. 1900-1918.

Hodgson, D.M., Flint, S.S., Hodgetts, D., Drinkwater, N.J., Johannessen, E.P., and Luthi, S., 2006, Stratigraphic evolution of fine-grained submarine fan systems, Tanqua depocentre, Karoo Basin, South Africa: Journal of Sedimentary Research, v. 76, p. 20– 40.

Hodgson, D.M., 2009, Distribution and origin of hybrids beds in sand-rich submarine fans of the Tanqua depocentre, Karoo Basin, South Africa: Marine and Petroleum Geology, v. 26, p. 1940-1956.

Hodgson, D.M., Kane, I.A., Flint, S.S., Brunt, R.L. and Ortiz-Karpf, A., 2016, Time-transgressive confinement on the slope and the progradation of basin-floor fans: Implications for the sequence stratigraphy of deep-water deposits: Journal of Sedimentary Research, v. 86, p.73-86.

Hofstra, M., Hodgson, D.M., Peakall, J., and Flint, S.S., 2015, Giant-scour fills in ancient channel-lobe transition zones: Formative processes and depositional architecture: Sedimentary Geology, v. 329, p. 98-114.

Hunter, R.E., 1977, Terminology of cross-stratified sedimentary layers and climbing-ripple structures: Journal of Sedimentary Research, v. 47, p. 697–706.

Ito, M., 2008, Downfan Transformation from turbidity currents to debris flows at a channel-to-lobe transitional zone: The Lower Pleistocene Otadai Formation, Boso Peninsula, Japan: Journal of Sedimentary Research, v. 78, p. 668-682.

Iverson, R.M., 1997, The physics of debris flow: Reviews of Geophysics, *v.* 35, p. 245-296.

Jegou, I., Savoye, B., Pirmez, C., and Droz, L., 2008, Channel-mouth lobe complex of the recent Amazon fan: The missing piece: Marine Geology, v. 252, p. 62–77.

Jobe, Z.R., Lowe, D.R., Morris, W.R., 2012, Climbing-ripple successions in turbidite systems: depositional environments, sedimentation rates and accumulation times: Sedimentology, v. 59, p. 867-898.

Johnson, S.D., Flint, S.S., Hinds, D., and Wickens, H.d.V., 2001, Anatomy of basin floor to slope turbidite systems, Tanqua Karoo, South Africa: sedimentology, sequence stratigraphy and implications for subsurface prediction: Sedimentology, v. 48, p. 987–1023.

Jopling, A.V., and Walker, R.G., 1968, Morphology and origin of ripple-drift cross-lamination, with examples from the Pleistocene of Massachusetts: Journal of Sedimentary Petrology, v. 38, p. 971–984.

Kane, I.A. and Pontén, A.S.M., 2012, Submarine transitional flow deposits in the Paleogene Gulf of Mexico: Geology, *v.* 40, p. 1119-1122.

Kane, I., Pontén, A., Vangdal, B., Eggenhuisen, J., Hodgson, D.M. and Spychala, Y.T., accepted, The stratigraphic record and processes of turbidity current transformation across deep-marine lobes: Sedimentology. DOI: 10.1111/sed.12346

Kneller, B.C., and Branney, M.J., 1995, Sustained high-density turbidity currents and the deposition of thick massive sands: Sedimentology, v. 42, p. 607-616.

Leclair, S.F., and Arnott, R.W.C., 2005, Parallel Lamination Formed by High-Density Turbidity Currents: Journal of Sedimentary Research, v. 75, p. 1-5.

Levorsen, A.I., 1936, Structural versus structural accumulation: American Association of Petroleum Geologists, Bulletin, v. 20, p. 521-530.

Lowe, D.R., 1982, Sediment gravity flows: II. Depositional models with special reference to the dposits of high-density turbidity currents: Journal of Sedimentary Petrology, v. 52, p. 279-297.

Lowe, D.R., and Guy, M., 2000, Slurry-flow deposits in the Britannia Formation (Lower Cretaceous), North Sea: a new perspective on the turbidity current and debris flow problem: Sedimentology, v. 47, p. 31-70.

Luthi, S., 1981, Experiments on non-channelized turbidity currents and their deposits: Marine Geology, v. 40, p. M59-M68.

Luthi, S.M., Hodgson, D.M., Geel, C.R., Flint, S.S., Goedbloed, J.W., Drinkwater, N.J., and Johannessen, E.P., 2006, Contribution of research borehole data to modelling fine-grained turbidite reservoir analogues, Permian Tanqua-Karoo basin-floor fans (South Africa): Petroleum Geosciences, v. 12, p. 175-190.

Macdonald, H.A., Peakall, J., Wignall, P.B., and Best, J., 2011, Sedimentation in deep-sea lobe elements: implications for the origin of the thickening-upward sequences: Geological Society of London, Journal, v. 168, p. 319-331.

MacPherson, B.A., 1978, Sedimentation and Trapping Mechanism in Upper Miocene Stevens and older turbidite fans of Southeastern San Joaquin Valley, California: American Association of Petroleum Geologists, Bulletin, *v.* 62, p. 2243-2274.

Marchand, A.M.E., Apps, G., Li, W., and Rotzien, J.R., 2015, Depositional processes and impact on reservoir quality in deepwater Paleogene reservoirs, US Gulf of Mexico: American Association of Petroleum Geologists, Bulletin, v. 99, p. 1635-1648.

Marini, M., Milli, S., and Moscatelli, M., 2011, Facies and architecture of the Lower Messinian turbidite complexes from the Laga Basin (central Apennines, Italy): Journal of Mediterranean Earth Science, v. 3, p. 45-72.

Marini, M., Salvatore, M., Ravnås, R., and Moscatelli, M., 2015, A comparative study of confined vs. semi-confined turbidite lobes from the Lower Messinian Laga Basin (Central Apennines, Italy): Implications for assessment of reservoir architecture: Marine and Petroleum Geology, v. 63, p. 142-165.

Masalimova, L.U., Lowe, D.R., Sharman, G.R., King, P.R., and Arnot, M.J., 2016, Outcrop characterization of a submarine channel-lobe complex: The Lower Mount Messenger Formation, Taranaki Basin, New Zealand: Marine and Petroleum Geology, v. 71, p.360-390.

McCave, I.N., and Jones, K.P.N., 1988, Deposition of ungraded muds from high-density non-turbulent turbidity currents: Nature, v. 333, p. 250-252.

Morris, W.R., Scheilhing, M.H., Wickens, DeV., Bouma, A.H., 2000, Reservoir architecture of deepwater sandstones: examples from the Skoorsteenberg Formation, Tanqua Karoo Sub-Basin, South Africa, *in* Weimer, P., Slatt, R.M., Bouma, A.H., and Lawrence, D.T., eds., Deep-Water Reservoirs of the World: Gulf Coast Section SEPM Foundation, Twentieth Annual Research Conference, p. 1010-1032.

Mutti, E., 1977, Distinctive thin-bedded turbidite facies and related depositional environments in the Eocene Hecho Group (South-central Pyrenees, Spain): Sedimentology, v. 24, p. 107-131.

Mutti, E., 1992, Turbidite Sandstones. Instituto di Geologia, Università di Parma & AGIP, San Donato Milanese, Italy, 275 p.

Nagatomo, A., and Archer, S., 2015, Termination geometries and reservoir properties of the Forties Sandstone pinch-out, East Central Graben, UK North Sea, *in* McKie, T., Rose, P.T.S., Hartley, A.J., Jones, D.W., and Armstrong, T.L., eds., Tertiary Deep-Marine Reservoirs of the North Sea Region: Geological Society of London, Special Publication,. 403, p. 133-155.

Nelson, C.H., Twichell, D.C., Schwab, W.C., Lee, H.J., and Kenyon, N.H., 1992, Upper Pleistocene turbidite sand beds and chaotic silt beds in the channelized, distal, outer-fan lobes of the Mississippi fan: Geology, v. 20, p. 693–696.

Normark, W.R., 1978, Fan valleys, channels, and depositional lobes on modern submarine fans: characters for recognition of sandy turbidite environments: American Association of Petroleum Geologists, Bulletin, v. 62, p. 912-931.

Patacci, M., Haughton, P.D.W., and McCaffrey, W.D., 2014, Rheological complexity in sediment gravity flows forced to decelerate against a confining slope, Braux, SE France: Journal of Sedimentary Research, v. 84, p. 270-277.

Pickering, K.T., 1981, Two types of outer fan lobe sequence, from the late Precambrian Kongsfjord Formation submarine fan, Finnmark, North Norway: Journal of Sedimentary Petrology, v. 51, p. 1277-1286.

Pickering, K.T., 1983, Transitional submarine fan deposits from the late Precambrian Kongsfjord Formation submarine fan, NE Finnmark, N. Norway: Sedimentology, v. 30, 181-199.

Piper, D.J.W., and Normark, W.R., 1983, Turbidite depositional patterns and flow characteristics, Navy Submarine Fan, California Borderland: Sedimentology, v. 30, p. 681-694.

Porten, K.W., Kane, I.A., Warchoł, M.J. and Southern, S.J., 2016, A sedimentological process-based approach to depositional reservoir quality of deep-marine sandstones: an example from the Springar Formation, north-western Vøring Basin, Norwegian Sea: Journal of Sedimentary Research, v. 86, 1269-1286.

Prélat, A., Hodgson, D.M., and Flint, S.S., 2009, Evolution, architecture and hierarchy of distributary deep-water deposits: a high-resolution outcrop investigation from the Permian Karoo Basin, South Africa: Sedimentology, v. 56, p. 2132-2154.

Prélat, A., Covault, J.A., Hodgson, D.M., Fildani, A., and Flint S.S., 2010, Intrinsic controls on the range of volumes, morphologies, and dimensions of submarine lobes: Sedimentary Geology, v. 232, p. 66-76.

Prélat, A., and Hodgson, D.M., 2013, The full range of turbidite bed thickness patterns in submarine lobes: controls and implications: Geological Society of London, Journal, v. 170, p. 1-6.

Pysklywec, R.N., and Mitrovica, J.X., 1999, The role of subduction-induced subsidence in the evolution of the Karoo Basin: The Journal of Geology, v. 107, p. 155-164.

Rittenhouse, G., 1972, Stratigraphic-trap classification: Geologic exploration methods, *in* Gould, H.R., ed., Stratigraphic Oil and Gas Fields—Classification, Exploration Methods, and Case Studies: American Association of Petroleum Geologists, Memoir, 16, p. 14-28.

Rozman, D.J., 2000, Characterization of a fine-grained outer submarine fan deposit, Tanqua-Karoo Basin, South Africa , *in* Bouma, A.H., and Stone, C.G., eds., Fine-Grained Turbidite Systems: American Association of Petroleum Geologists, Memoir 72/SEPM, Special Publication, 68, p. 279-290.

Saller, A., Werner, K., Sugiaman, F., Cebastiant, A., May, R., Glenn, D., and Barker, C., 2008, Characteristics of Pleistocene deep-water fan lobes and their application to an upper Miocene reservoir model, offshore East Kalimantan, Indonesia: American Association of Petroleum Geologists, Bulletin, v. 92, p. 919–949.

Smith, R., 1987a, Structure and deformation history of the Central Wales Synclinorium, northeast Dyfed: evidence for a long-lived basement structure: Geological Journal, *v.* 22, p.183-198.

Smith, R., 1987b, The *Griestoniensis* Zone Turbidite System, Welsh Basin, in Leggett, J.K. and Zuffa, C.G., eds., Marine Clastic Sedimentology: Concepts and Case Studies: London, Graham & Trotman, p. 89-107.

Smith, R., 2004, Turbidite systems influenced by structurally induced topography in the multi-sourced Welsh Basin, *in* Lomas, S.A., and Joseph, P., eds., Confined Turbidite Systems: Geological Society of London, Special Publication, 222, p. 209-228.

Smith, R., and Joseph, P., 2004, Onlap stratal architectures in the Gres d'Annot: geometric models and controlling factors, *in* Joseph, P. and Lomas, S.A., eds., Deep-Water Sedimentation in the Alpine

Basin of Se France: New Perspectives on the Gres d'Annot and Related Systems: Geological Society of London, Special Publication, 221, p. 389-399.

Sømme, T.O., Helland-Hansen, W., Martinsen, O., and Thurmond, J.B., 2009, Relationships between morphological and sedimentological parameters in source-to-sink systems: a basis for predicting semi-quantitative characteristics in subsurface systems: Basin Research, v. 21, p. 361–387.

Southard, J.B., 1991, Experimental determination of bed-form stability: Annual Review of Earth and Planetary Science, v. 19, p. 423-455.

Southern, S.J., Patacci, M., Felletti, F., and McCaffrey, W.D., 2015, Influence of flow containment and substrate entrainment upon sandy hybrid event beds containing a co-genetic mud-clast rich division: Sedimentary Geology, *v.* 321, p. 105-122.

Southern, S.J., Kane, I.A., Warchoł, M.J., Porten, K.W. and McCaffrey, W.D., 2016, Hybrid event beds dominated by transitional-flow facies: Character, distribution and significance in the Maastrichtian Springar Formation, north-west Vøring Basin, Norwegian Sea. Sedimentology, published online. DOI: 10.1111/sed.12323

Spychala, Y.T., Hodgson, D.M., Flint, S.S., and Mountney, N.P., 2015, Constraining the sedimentology and stratigraphy of submarine intraslope lobe deposits using exhumed examples from the Karoo Basin, South Africa: Sedimentary Geology, v. 322, p. 67-81.

Spychala, Y.T., Hodgson, D.M., Stevenson, C.J., and Flint, S.S., 2016, Aggradational lobe fringes: the influence of subtle intrabasinal topography on sediment gravity flow processes and lobe stacking patterns: Sedimentology, published online. DOI: 10.1111/sed.12315

Stow, D.A.V., Piper, D.J.W., 1984, Deep-water fine-grained sediments: facies models. *in* Stow, D.A.V., Piper, D.J.W., eds., Fine-Grained Sediments: Deep-water Processes and Facies. Geological Society of London, Special Publication, 15, p. 611-646.

Talling, P.J., Amy, L.A., Wynn, R.B., Peakall, J., and Robinson, M., 2004, Beds comprising debrite sandwiched within co-genetic turbidite: origin and widespread occurrence in distal depositional envrionments: Sedimentology, v. 51, p. 163-194.

Talling, P.J., Masson, D.G., Sumner, E.J., and Malgesini, G., 2012a, Subaqueous sediment density flows: Depositional processes and deposit types: Sedimentology, v. 59, p. 1937-2003.

Talling, P.J., Malgesini, G., Sumner, E.J., Amy, L.A., Felletti, F., Blackbourn, G., Nutt, C., Wilcox, C., Harding, I.C., and Akbari, S., 2012b, Planform geometry, stacking pattern, and extrabasinal origin of low strength and intermediate strength cohesive debris flow deposits in the Marnoso-arenacea Formation, Italy: Geosphere, v. 8, p. 1207-1230.

Talling, P.J., 2013, Hybrid submarine flows comprising turbidity current and cohesive debris flow: Deposits, theoretical and experimental analyses, and generalized models: Geosphere, v. 9, p. 460-488.

Tankard, A., Welsink, H., Aukes, P., Newton, R., and Stettler, E., 2009, Tectonic evolution of the Cape and Karoo basins of South Africa: Marine and Petroleum Geology, v. 26, p. 1379-1412.

Twichell, D.C., Schwab, W.C., Nelson, C.H., Kenyon, N.H., and Lee, H.J., 1992, Characteristics of a sandy depositional lobe on the outer Mississippi fan from DeaMARC IA sidescan sonar images: Geology, v. 20, p. 689–692.

Twichell, D.C., Cross, V.A., Hanson, A.D., Buck, B.J., Zybala, J.G., and Rudin, M.J., 2005, Seismic architecture and lithofacies of turbidites in Lake Mead (Arizona and Nevada, U.S.A.), an analogue for topographic complex basins: Journal of Sedimentary Research, *v.* 75, p. 134-148.

van der Werff, W., and Johnson, S., 2003a, High resolution stratigraphic analysis of a turbidite system, Tanqua Karoo Basin, South Africa: Marine and Petroleum, Geology, v. 20, p. 45-69.

van der Werff, W., and Johnson, S., 2003b, Deep-sea fan pinch-out geometries and their relationship to fan architecture, Tanqua Karoo basin (South Africa): Geologische Rundschau, v. 92, p. 728-742.

Visser, J.N.J, and Prackelt, H.E., 1996, Subduction, mega-shear systems and Late Palaeozoic basin development in the African segment of Gondwana: Geologische Rundschau, v. 85, p. 632-646.

Visser, J.N.J., 1997, Deglaciation sequences in the Permo-Carboniferous Karoo and Kalahari basins of the southern Africa: a tool in the analysis of cyclic glaciomarine basin fills: Sedimentology, v. 44, p. 507-521.

Wickens, H.d.V., 1994, Basin floor fan building turbidites of the southwestern Karoo Basin, Permian Ecca Group. PhD Thesis, Port Elizabeth University, South Africa, 233 p.

Wickens, H.d.V., and Bouma, A.H., 2000, The Tanqua Fan Complex, Karoo Basin, South Africa – outcrop analogue for fine-grained, deepwater deposits, *in* Bouma, A.H., and Stone, C.G., eds., Fine-

Grained Turbidite Systems , American Association of Petroleum Geologists, Memoir 72/SEPM, Special Publication, 68, p. 153–165.

Wild, R.J., Hodgson, D.M., and Flint, S.S., 2005, Architecture and stratigraphic evolution of multiple, vertically-stacked slope-channel complexes, Tanqua depocentre, Karoo Basin, South Africa, *in* Hodgson, D.M., and Flint, S.S., eds*.,* Submarine Slope Systems, Processes and Products: Geological Society of London, Special Publication, 244, p. 89–112.

Wild, R., Flint, S.S., and Hodgson, D.M., 2009, Stratigraphic evolution of the upper slope and the shelf edge in the Karoo Basin, South Africa: Basin Research, v. 21, p. 502-527.

Wilson, D., Davies, J.R., Waters, R.A., and Zalasiewicz, J.A., 1992, A fault-controlled depositional model for the Aberystwyth Grits turbiditic system: Geological Magazine, v. 129, p. 595-607.

Wynn, R.B., Weaver, P.E., Masson, D.G., and Stow, D.A.V., 2002, Turbidite depositional architecture across three interconnected deep-water basins on the north-west African margin: Sedimentology, v. 49, p. 669-695.

Figure Captions

Fig. 1: A) Simplified model indicating the various sub-environments in a lobe (redrawn from Prélat et al., 2009). B) Plan-form view of five-fold lobe hierarchy: bed to bed set, lobe element, lobe, lobe complex and lobe complex set (modified from Prélat et al., 2010).

Fig. 2: A) The Tanqua depocentre inboard of the Cape Fold Belt (Cederberg and Swartberg branches). The square indicates the location of the study area. B) Stratigraphy of the Tanqua depocenter (redrawn after Wild et al., 2009). The Skoorsteenberg Formation overlies the Tierberg Formation,

and is overlain by the Kookfontein Formation. This study focuses on Fan 4. Images taken from Google Earth.

Fig. 3: Locations of recently cored wells, outcrops, NOMAD well locations used in the study. Fan 4 outcrops are marked in white. Images taken from Google Earth.

Fig. 4: Representative outcrop photographs of observed sedimentary facies. A) Structureless thick-bedded sandstone (F1). Person for scale (~ 1.7 m); B) Structured medium-bedded sandstone (F2). C) Hybrid bed (F4) with lower clean division and upper mudstone clast –rich division, Lens cover as scale (~ 7 cm diameter); D) Thin-bedded heterolithic strata (F6). Logging pole for scale (10 cm increments); E) Thin-bedded siltstone (F7) and mudstone. Lens cover for scale (~ 7 cm diameter); F) Mudstone (F8) horizon overlain by sandstone. Logging pole for scale (10 cm increments).

Fig. 5: Representative core photographs of observed facies. A) Structureless sandstone (F1); B) Structured sandstone (F2); C) Banded sandstone (F3); D) Hybrid bed (F4) with lower clean sandstone division and upper argillaceous sandstone division; E) Debrites (F5); F) Heterolithic package (F6); G) Siltstones (F7); H) mudstone (F8).

Fig. 6: Isopach and paleocurrent maps for A) Lower and B) Upper Fan 4. Contours are in meters. Paleocurrent roses represent data collected during the study, whereas paleocurrent arrows represent data from previous work based on Hodgson et al. (2006).

Fig. 7: Correlation panels of Fan 4. Top: Correlation of a S-N transect from Bloukop (BK) to Isle of Sky (Ios). Bottom: SW-NE correlation from Klipfontein (Kf) to Isle of Sky (Ios). The base of the mudstone and siltstone interval (black unit) that separates the Lower and Upper Fan 4 is used as a datum. Pinchout of lobes 1-5 of the lower Fan 4 are indicated by black arrows, and their plan-view distribution is shown in Figure 10.

Fig. 8: A) Hierarchical model of Fan 4. Location of panel is marked in Fig. 3. Fan 4 consists of two sand-prone divisions that are separated by a thin-bedded heterolithic lobe fringe complex (LC2).

Lower Fan 4 comprises one lobe complex (LC1), and upper Fan 4 comprises two lobe complexes (LC3 and LC5) and a lobe complex fringe (LC4). Blue square marks zoom-in area of parts B and C. B) Close-up of the LC2 deposits in the OR well (see Fig. 3 for location). C) Corresponding core photographs.

Fig. 9: Representative photographs of lobe successions in the field area. A) Lobe fringe deposits of lower Fan 4 overlain by lobe axis and off-axis deposits of upper Fan 4. Person as scale (~1.7 m); B) Lobe fringe deposits of lower Fan 4 overlain by lobe axis and off-axis deposits of upper Fan 4 C) Lower Fan 4. Hybrid beds are separated by thin-bedded siltstone successions. Person as scale (~1.7 m). D) Thick-bedded lobe axis deposits of upper Fan 4. Person as scale (~ 1.7 m).

Fig. 10: Facies distributions and paleogeographic reconstruction for Lower Fan 4, which comprises one lobe complex (LC1) that prograded northward. Black lines indicate the location of lobe-scale dip and strike correlation panels in Figure 12. The green line indicates the location of the Los Kop outcrop area of Hodgson et al. (2006), whereas blue and purple lines mark the location of correlation panels in Figure 7, as do lobe numbers.

Fig. 11: Well-core log through Fan 4(NS3; see Fig. 2). The lower lobe complex of Fan 4 comprises solely thin-bedded heterolithic deposits, siltstones, and mudstones, which represents stacked lateral lobe fringe successions. The upper division of Fan 4 shows consists of interbedded structureless sandstone, hybrid beds and heterolithic packages.

Fig. 12: Dip and strike facies transitions in individual lobes within LC1 of Fan 4. A) Strike section in the Gemsbok Valley (see Figure 10 for location). Lithology changes from structureless sandstone to structured sandstone to heterolithic deposits. B) Dip section on the Sout Rivier area (see Figure 10 for location). Lithology is dominated by structureless sandstone, hybrid beds, and siltstone.

Fig. 13: Correlation panels of stacked frontal lobe fringes around Katjiesberg in LC3. A) Location of the correlation panels at Katjiesberg and paleogeography of the Upper Fan 4. B) Areal correlation of four pinch-out fingers and zoom into the northwestern-southeastern part of the correlation panel

with sedimentary facies of the pinch-out fingers. They are composed of structureless sandstone deposits, debrites, and siltstone deposits.

Fig. 14: Representative lobe fringe photographs. A) Frontal lobe fringe deposits at Katjiesberg. B) Frontal lobe fringe deposits at Katjiesberg. C) Lateral lobe fringe deposits at Klipfontein. Logging pole for scale. D) Lateral lobe fringe deposits at Hammerkranz. Logging pole for scale.

Fig.15: A) Simplified anatomy of frontal lobe fringe deposits. B) Simplified anatomy of lateral lobe fringe deposits. C) Example log showing a vertical section through a frontal lobe fringe in the Sout Rivier area. D) Example log showing a vertical section through a lateral lobe fringe in the Gemsbok East core.

Fig. 16 A) Simplified plan view of a lobe marking the distribution of lobe sub-environments and example logs for each sub-environment. B) Dominant flow processes to deposit frontal lobe fringes: High-density turbidity currents and strongly stratified flows. C) Low-density turbidity currents and debris flow deposit lateral lobe fringes. C is modified from Kane et al. (accepted).

Table 1. Summary of sedimentary facies of Fan 4.

Table 2. Recognition criteria of frontal and lateral lobes for outcrop and core.

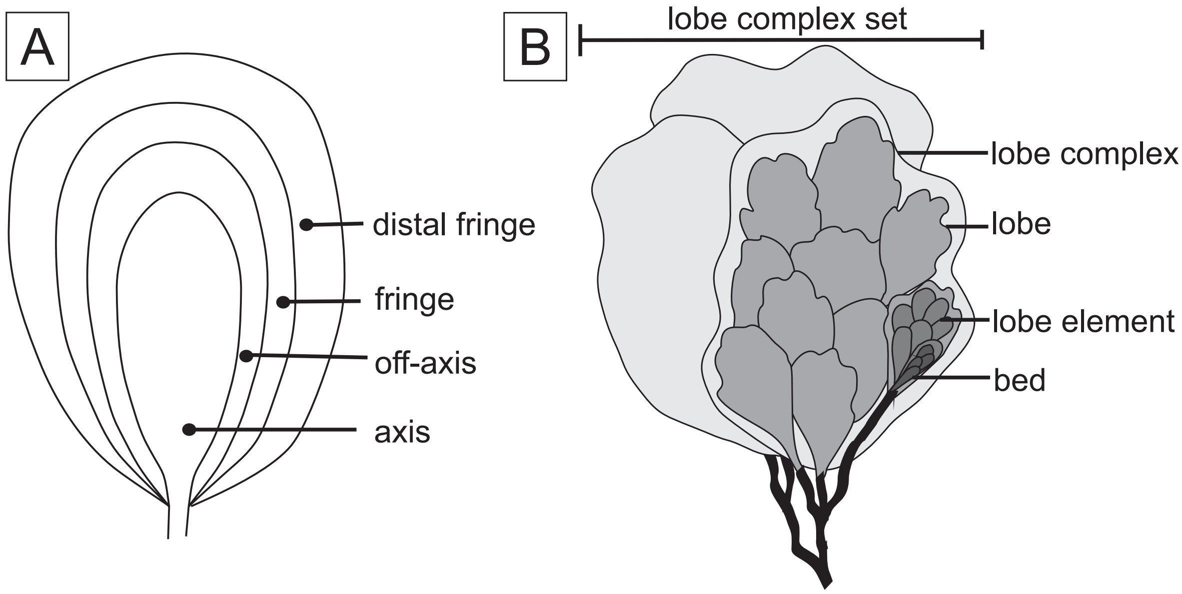
A
distal fringe
fringe
off-axis
axis
B
lobe complex set
lobe complex
lobe
lobe element
bed

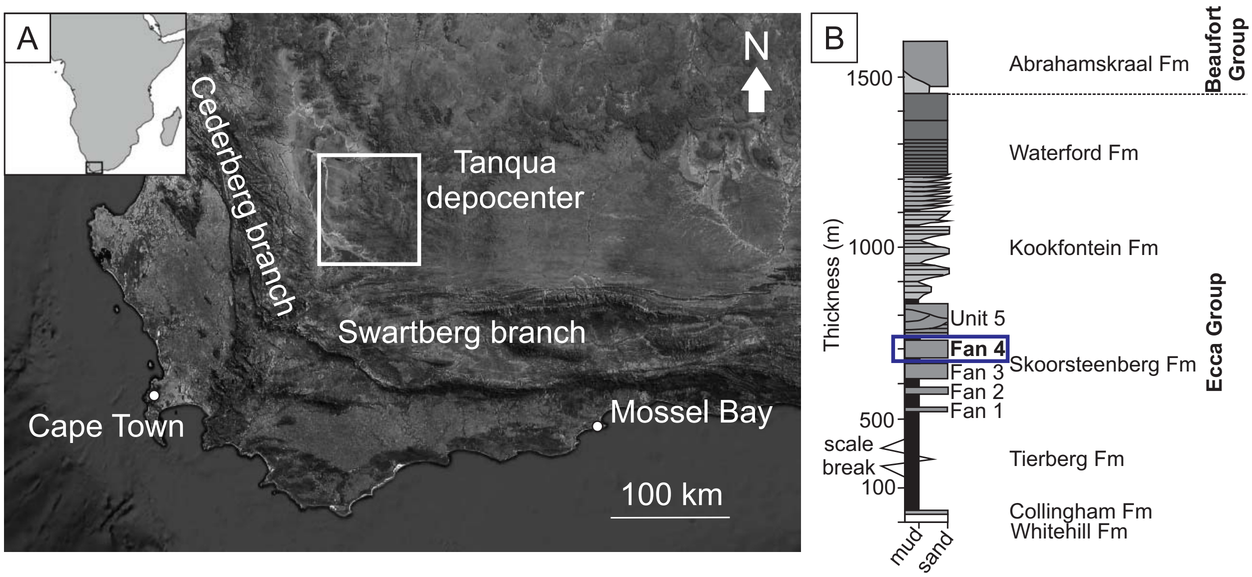
A
Cederberg branch
Tanqua
depocenter
Swartberg branch
Cape Town
Mossel Bay
100 km
N
B
Thickness (m)
1500
1000
500
100
scale
break
mud
sand
Abrahamskraal Fm
Beaufort Group
Waterford Fm
Kookfontein Fm
Unit 5
Fan 4
Fan 3
Fan 2
Fan 1
Skoorsteenberg Fm
Ecca Group
Tierberg Fm
Collingham Fm
Whitehill Fm

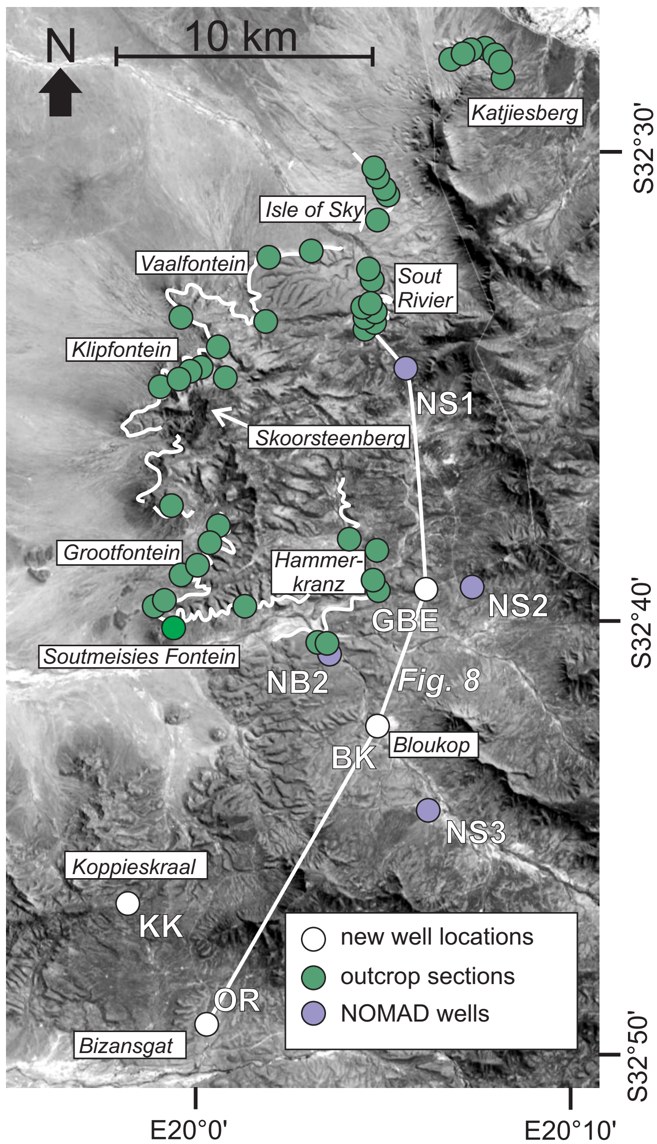

N
10 km
Katjiesberg
Isle of Sky
Vaalfontein
Sout
Rivier
Klipfontein
NS1
Skoorsteenberg
Grootfontein
Hammer-
kranz
GBE
NS2
Soutmeisies Fontein
NB2
Fig. 8
Bloukop
BK
NS3
Koppieskraal
KK
new well locations
outcrop sections
NOMAD wells
OR
Bizansgat
S32°30'
S32°40'
S32°50'
E20°0'
E20°10'

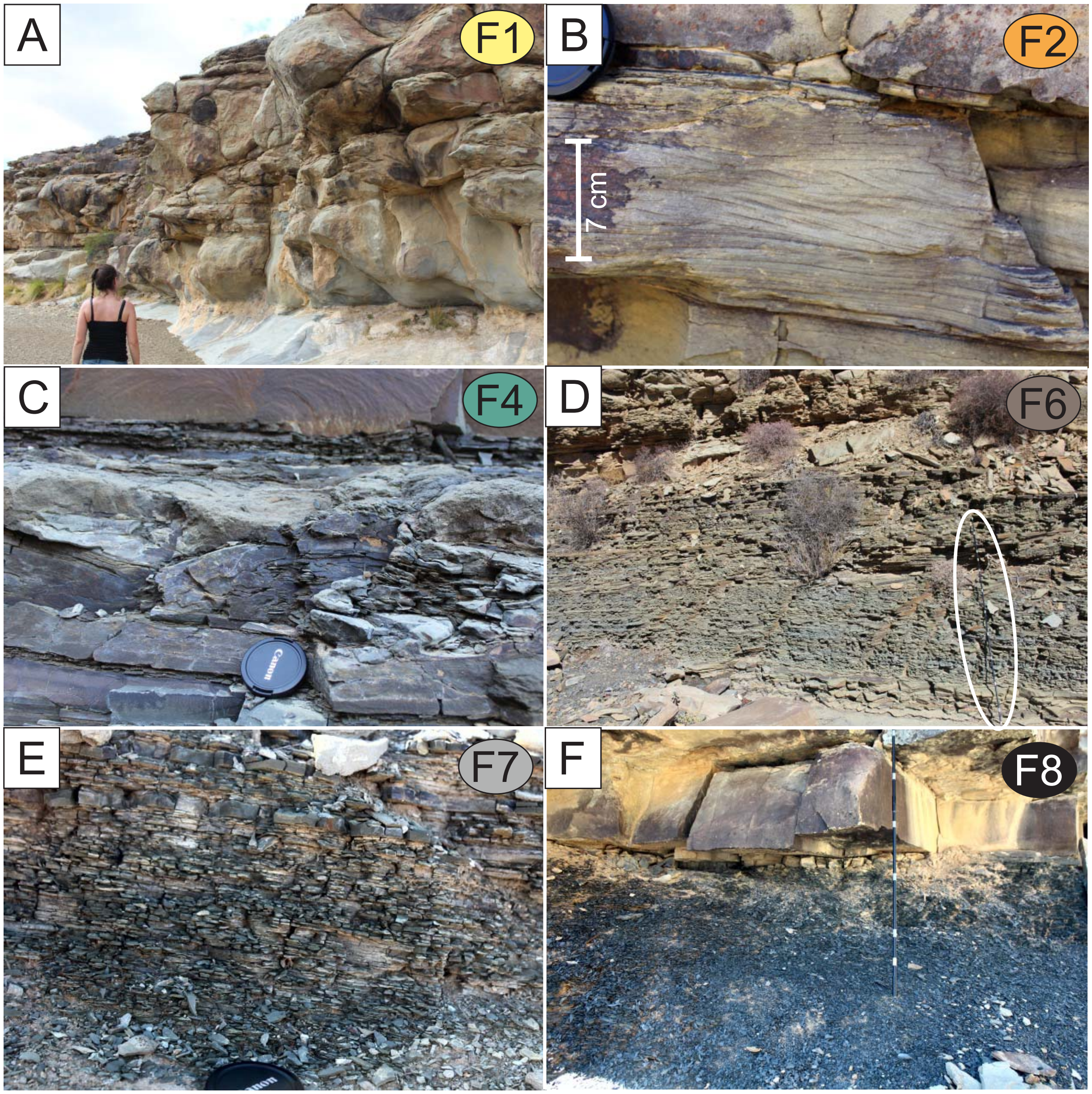
A
F1
B
F2
7 cm
C
F4
D
F6
E
F7
F
F8

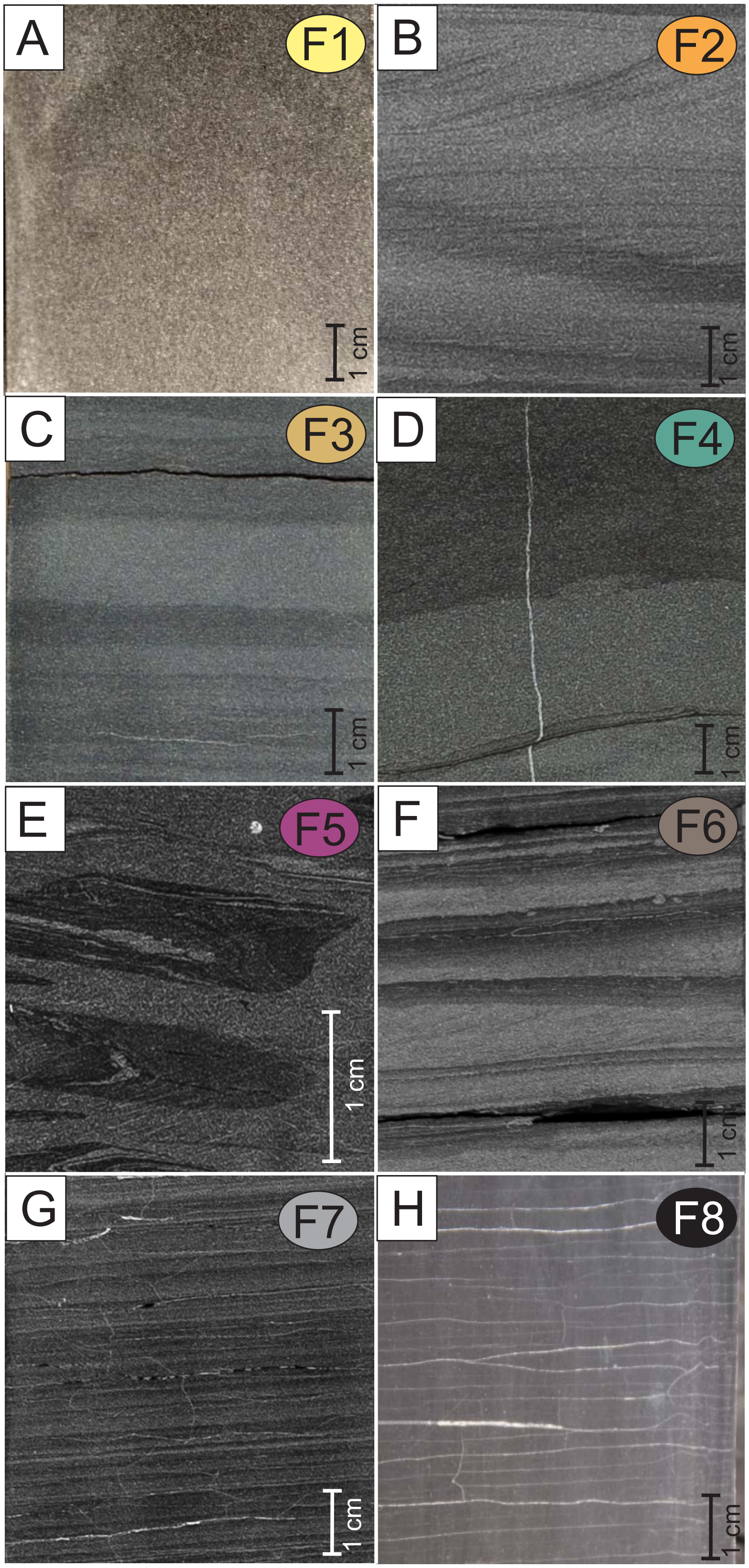

A
F1
1 cm
B
F2
1 cm
C
F3
1 cm
D
F4
1 cm
E
F5
1 cm
F
F6
1 cm
G
F7
1 cm
H
F8
1 cm

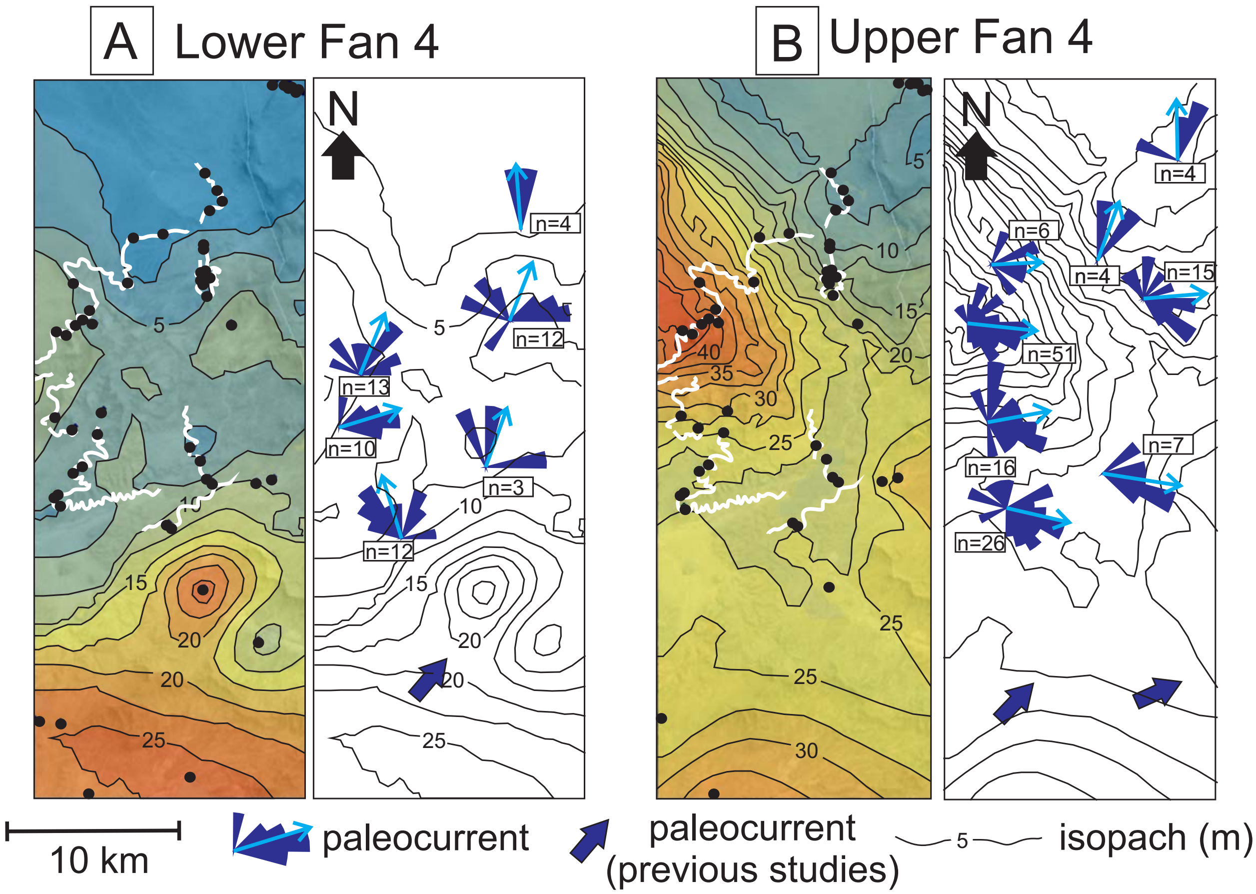
A Lower Fan 4
B Upper Fan 4
N
5
10
15
20
25
n=4
n=12
n=13
n=10
n=3
n=12
40
35
30
30
n=6
n=4
n=15
n=51
n=16
n=7
n=26
10 km
paleocurrent
paleocurrent
(previous studies)
isopach (m)

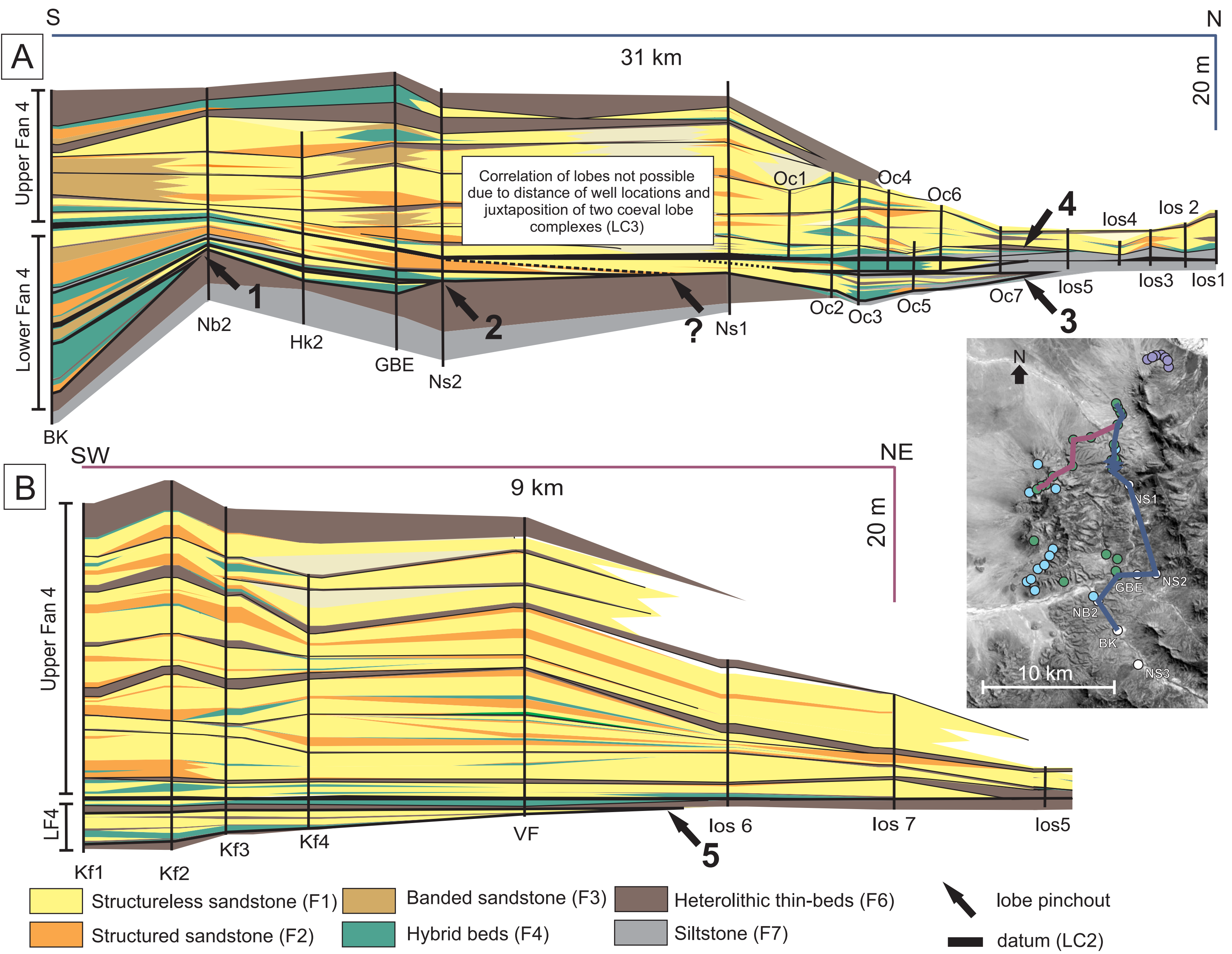

S
N
A
31 km
20 m
Upper Fan 4
Lower Fan 4
Correlation of lobes not possible due to distance of well locations and juxtaposition of two coeval lobe complexes (LC3)
BK
Nb2
Hk2
GBE
Ns2
Ns1
Oc1
Oc2
Oc3
Oc4
Oc5
Oc6
Oc7
Ios5
Ios4
Ios3
Ios 2
Ios1
1
2
?
3
4
N
NS1
NS2
GBE
NB2
BK
NS3
10 km
SW
NE
B
9 km
20 m
Upper Fan 4
LF4
Kf1
Kf2
Kf3
Kf4
VF
Ios 6
Ios 7
Ios5
5
Structureless sandstone (F1)
Structured sandstone (F2)
Banded sandstone (F3)
Hybrid beds (F4)
Heterolithic thin-beds (F6)
Siltstone (F7)
lobe pinchout
datum (LC2)

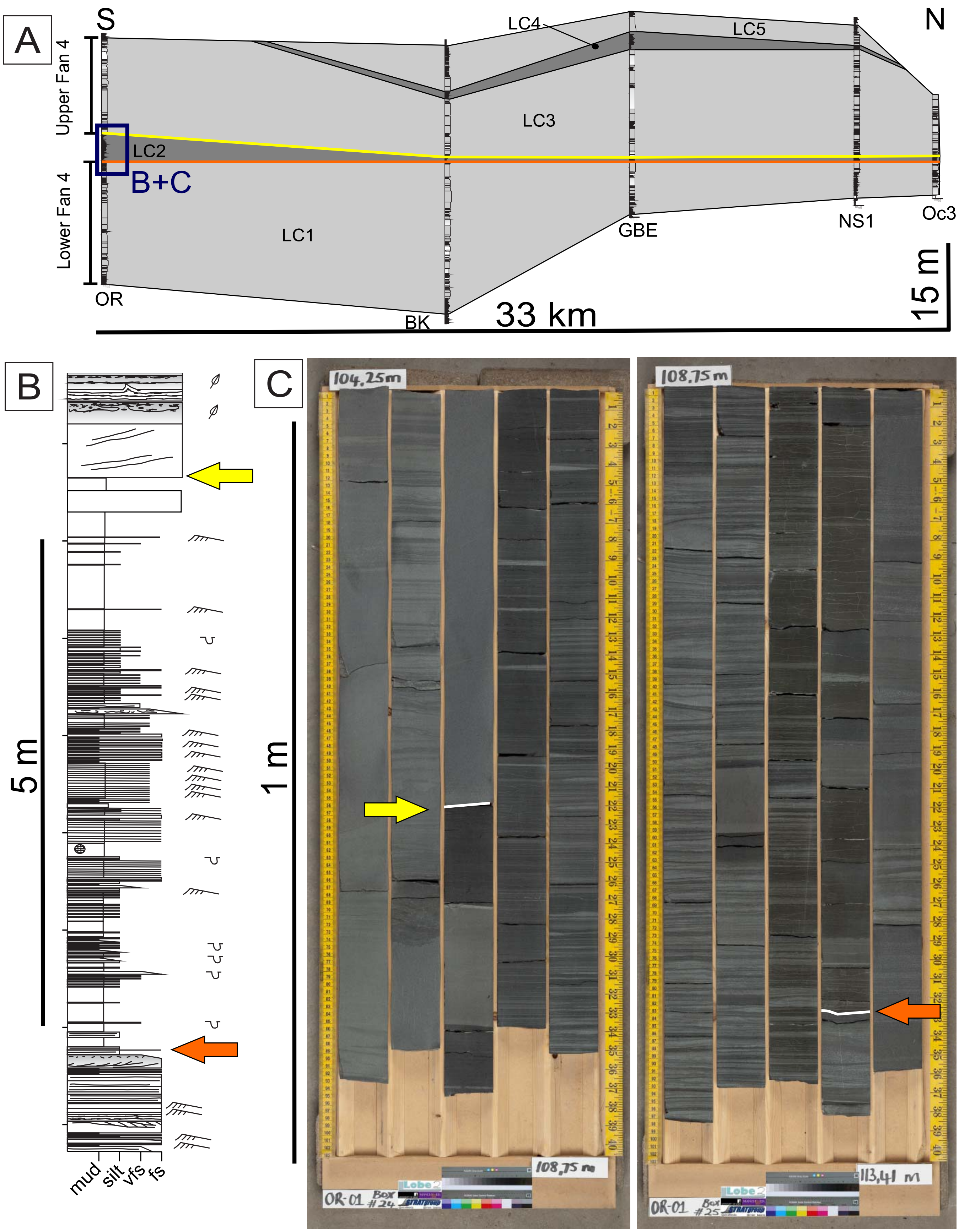
A
S
N
Upper Fan 4
Lower Fan 4
LC1
LC2
LC3
LC4
LC5
B+C
OR
BK
GBE
NS1
Oc3
33 km
15 m
B
5 m
mud
silt
vfs
fs
C
1 m
104,25m
108,75 m
108,75m
113,41 m
OR-01
Box #24
Box #25

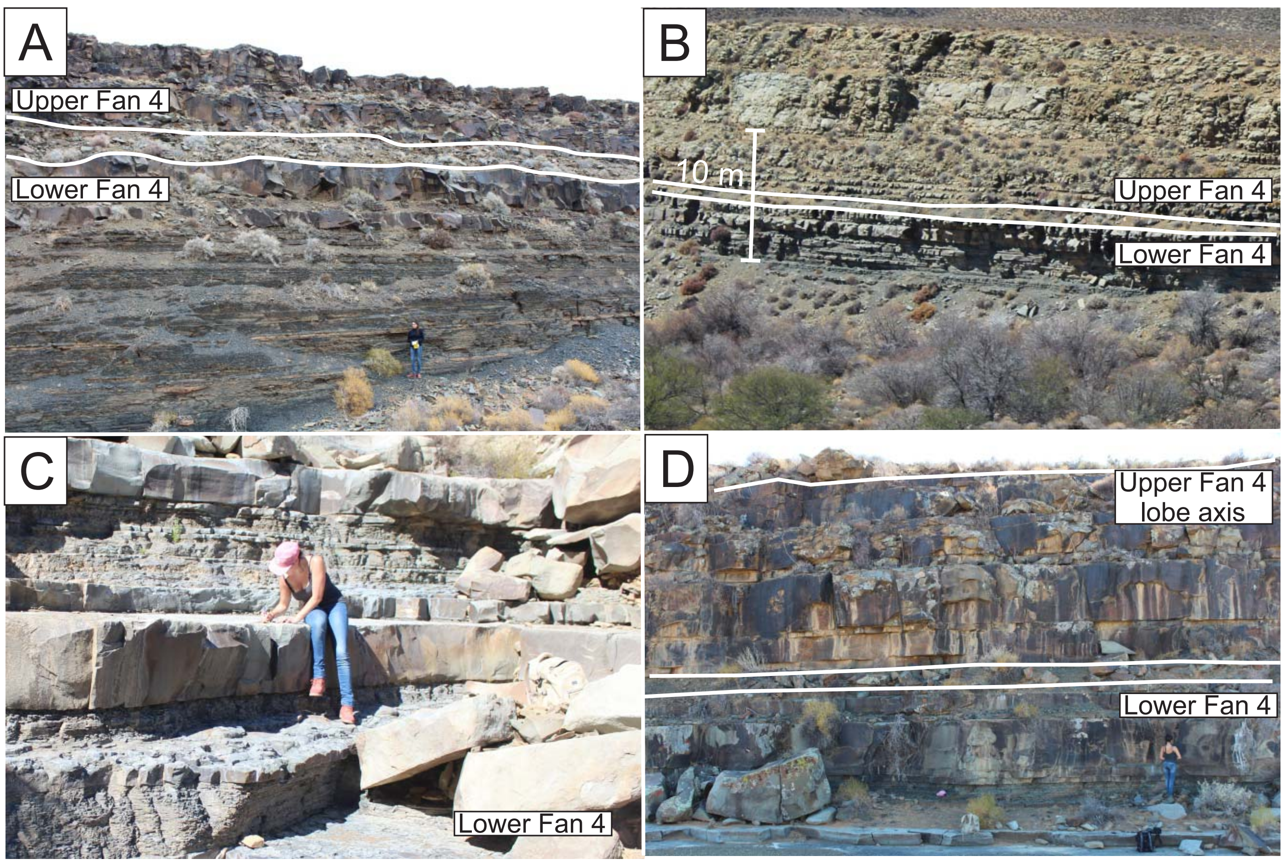
A
Upper Fan 4
Lower Fan 4
B
10 m
Upper Fan 4
Lower Fan 4
C
Lower Fan 4
D
Upper Fan 4
lobe axis
Lower Fan 4

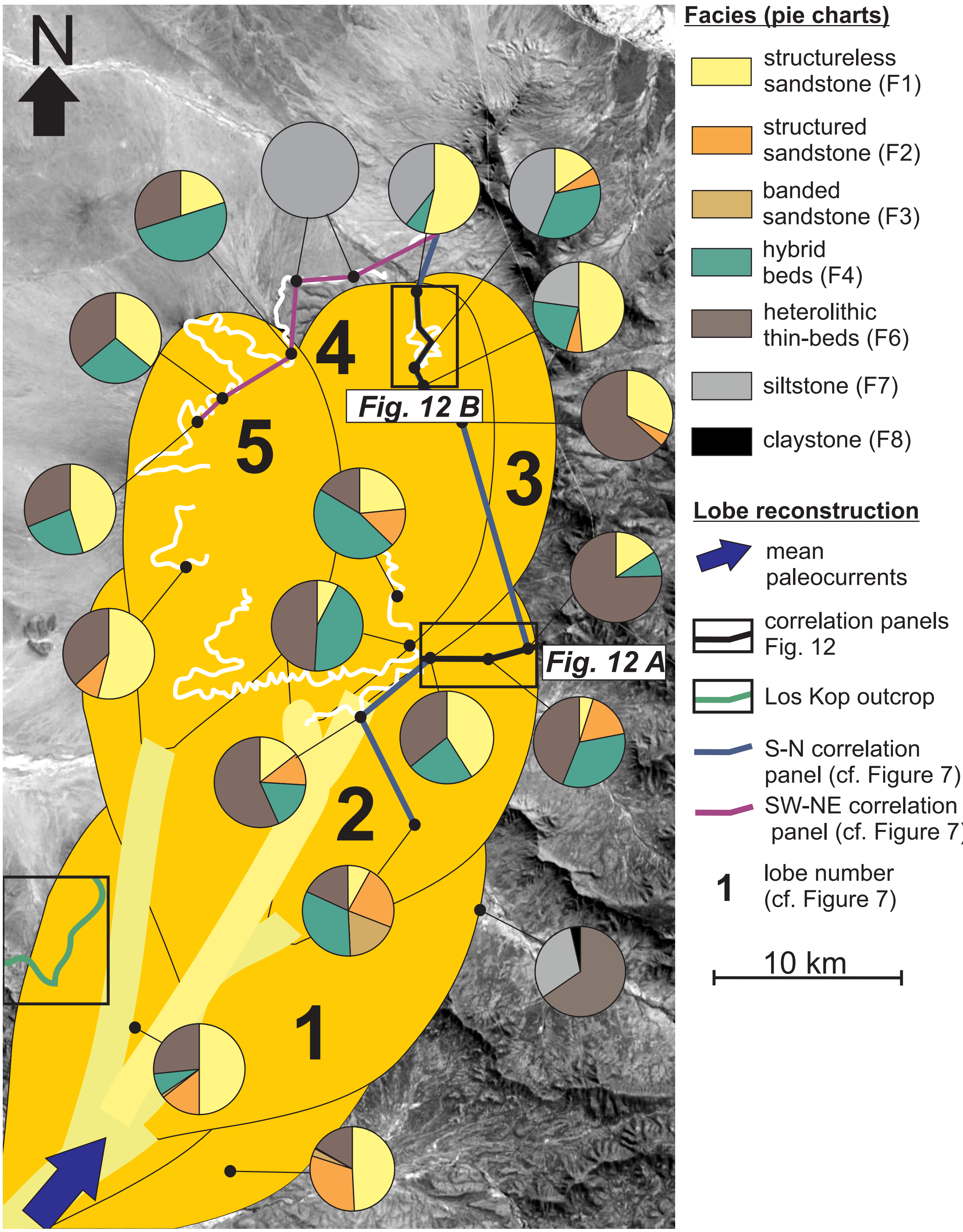

N
4
5
3
2
1
Fig. 12 B
Fig. 12 A
Facies (pie charts)
structureless sandstone (F1)
structured sandstone (F2)
banded sandstone (F3)
hybrid beds (F4)
heterolithic thin-beds (F6)
siltstone (F7)
claystone (F8)
Lobe reconstruction
mean paleocurrents
correlation panels Fig. 12
Los Kop outcrop
S-N correlation panel (cf. Figure 7)
SW-NE correlation panel (cf. Figure 7)
1 lobe number (cf. Figure 7)
10 km

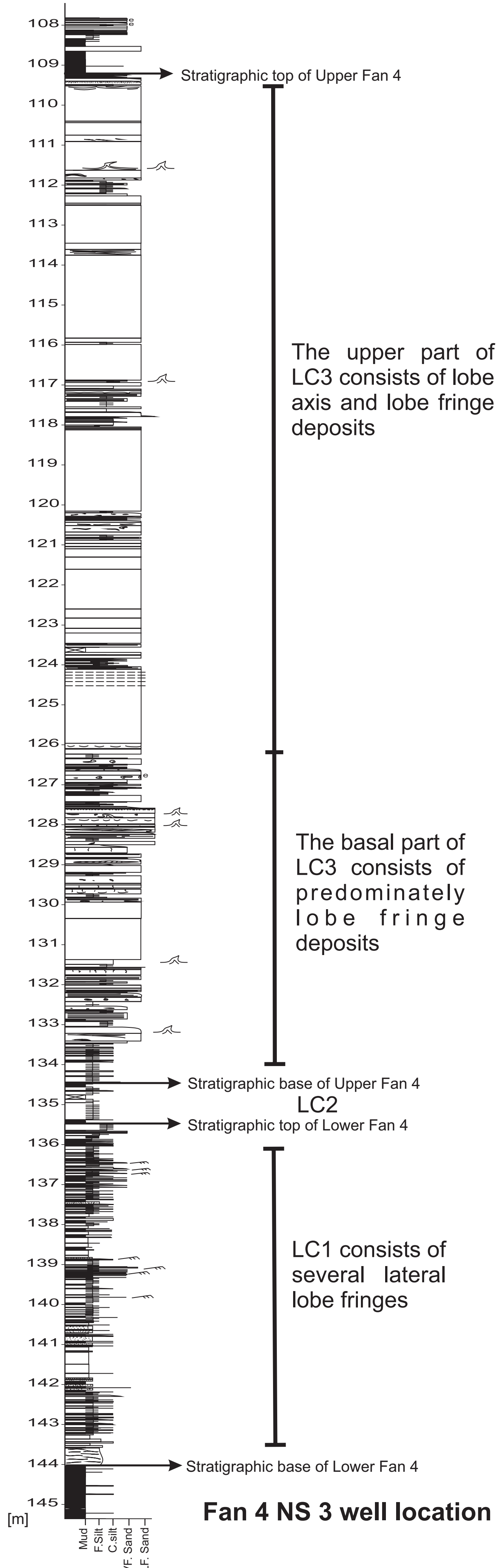

Fan 4 NS 3 well location

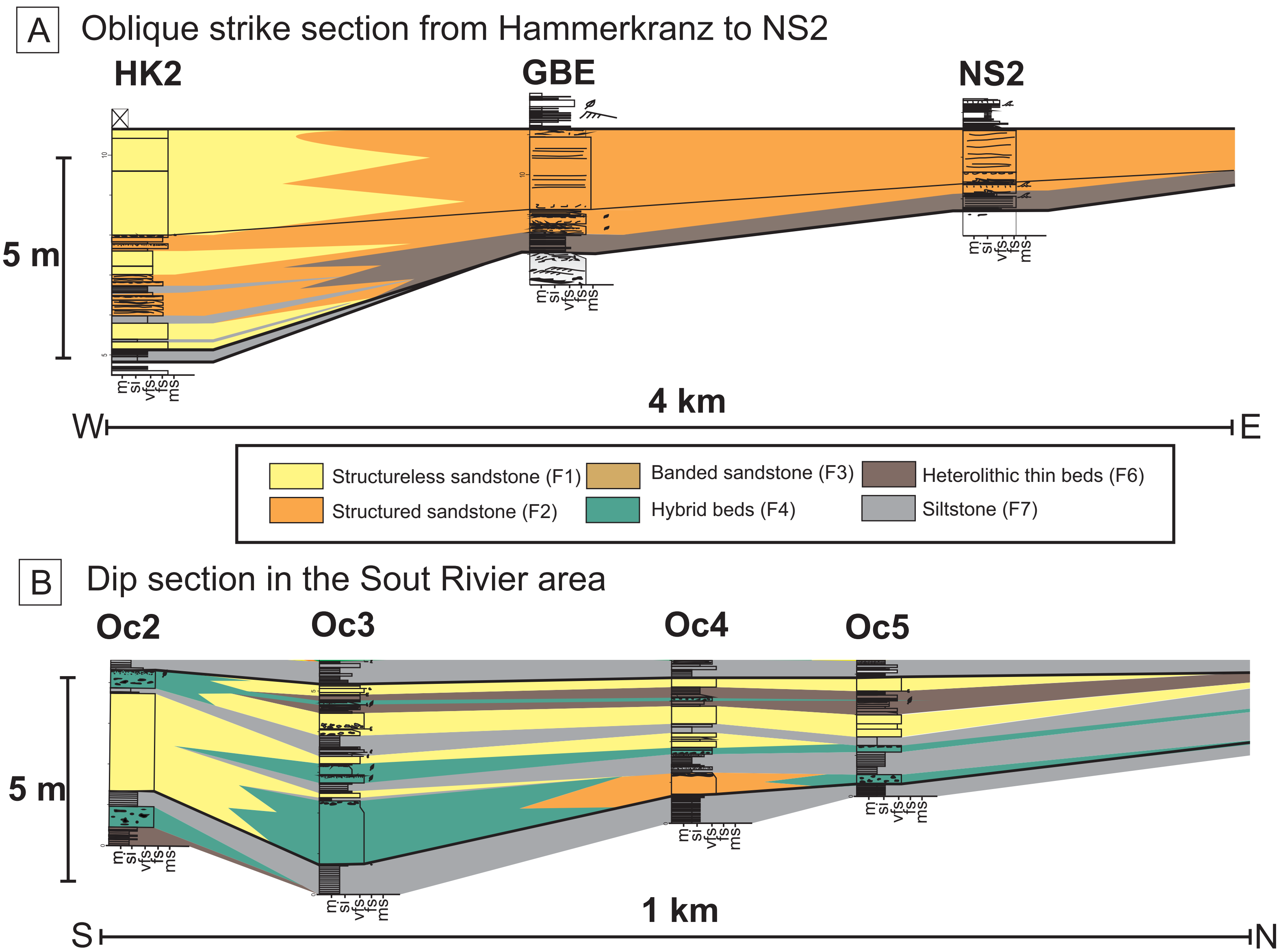

A
Oblique strike section from Hammerkranz to NS2
HK2
GBE
NS2
5 m
m
si
vfs
fs
ms
4 km
W
E
Structureless sandstone (F1)
Structured sandstone (F2)
Banded sandstone (F3)
Hybrid beds (F4)
Heterolithic thin beds (F6)
Siltstone (F7)
B
Dip section in the Sout Rivier area
Oc2
Oc3
Oc4
Oc5
5 m
1 km
S
N

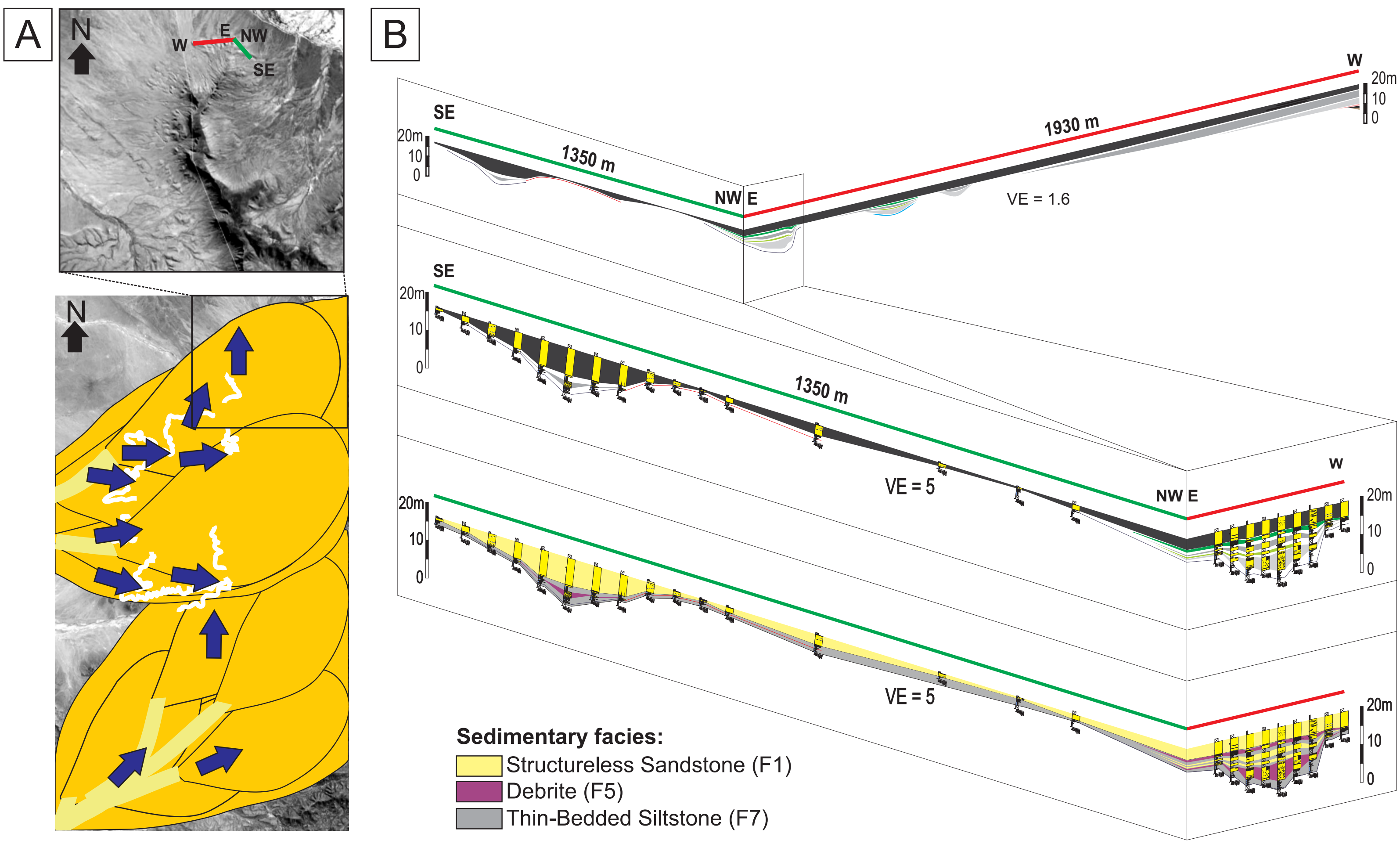

A
N
W
E
NW
SE
N
B
SE
20m
10
0
1350 m
NW
E
1930 m
W
20m
10
0
VE = 1.6
SE
20m
10
0
1350 m
VE = 5
NW
E
W
20m
10
0
20m
10
0
VE = 5
20m
10
0
Sedimentary facies:
Structureless Sandstone (F1)
Debrite (F5)
Thin-Bedded Siltstone (F7)

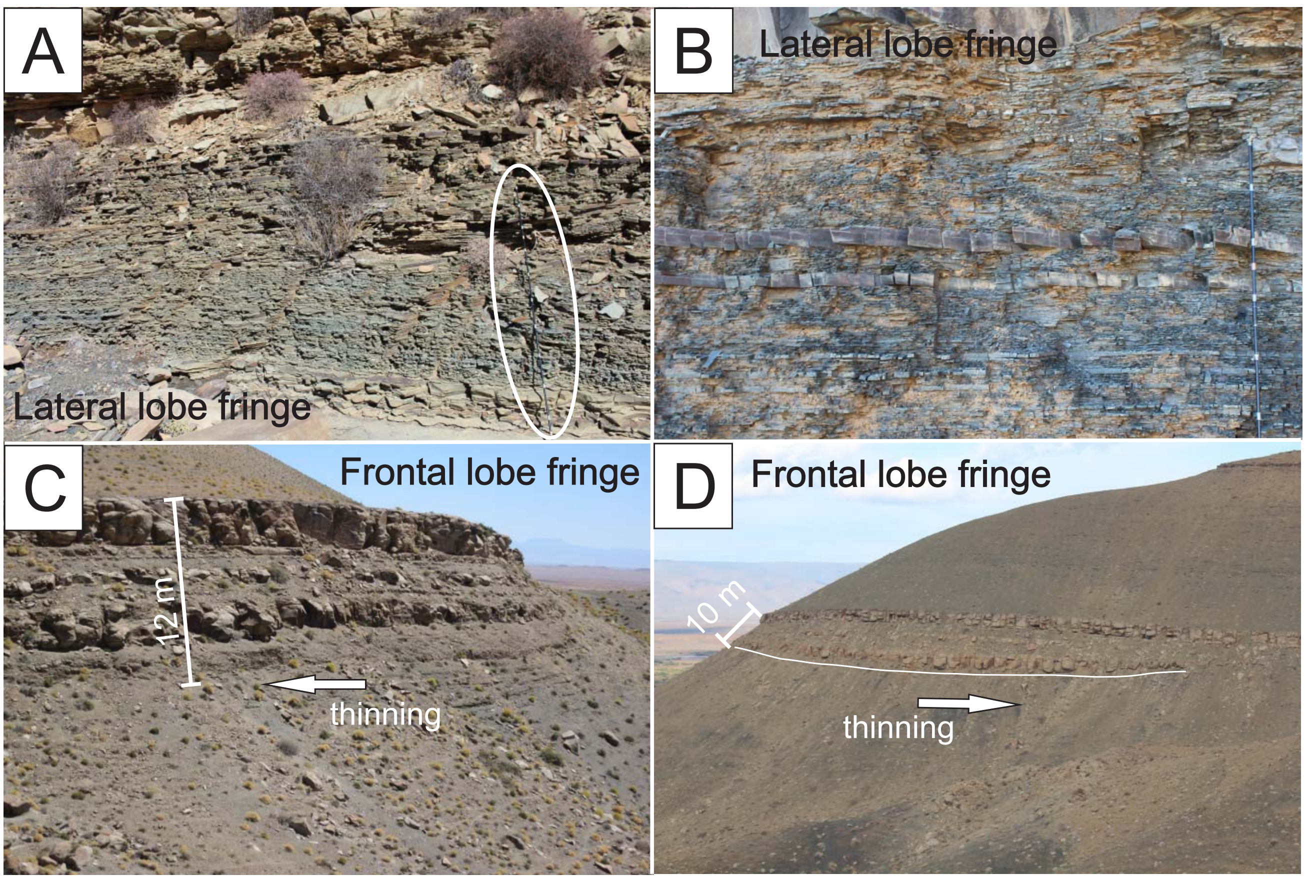
A
Lateral lobe fringe
B
Lateral lobe fringe
C
Frontal lobe fringe
12 m
thinning
D
Frontal lobe fringe
10 m
thinning

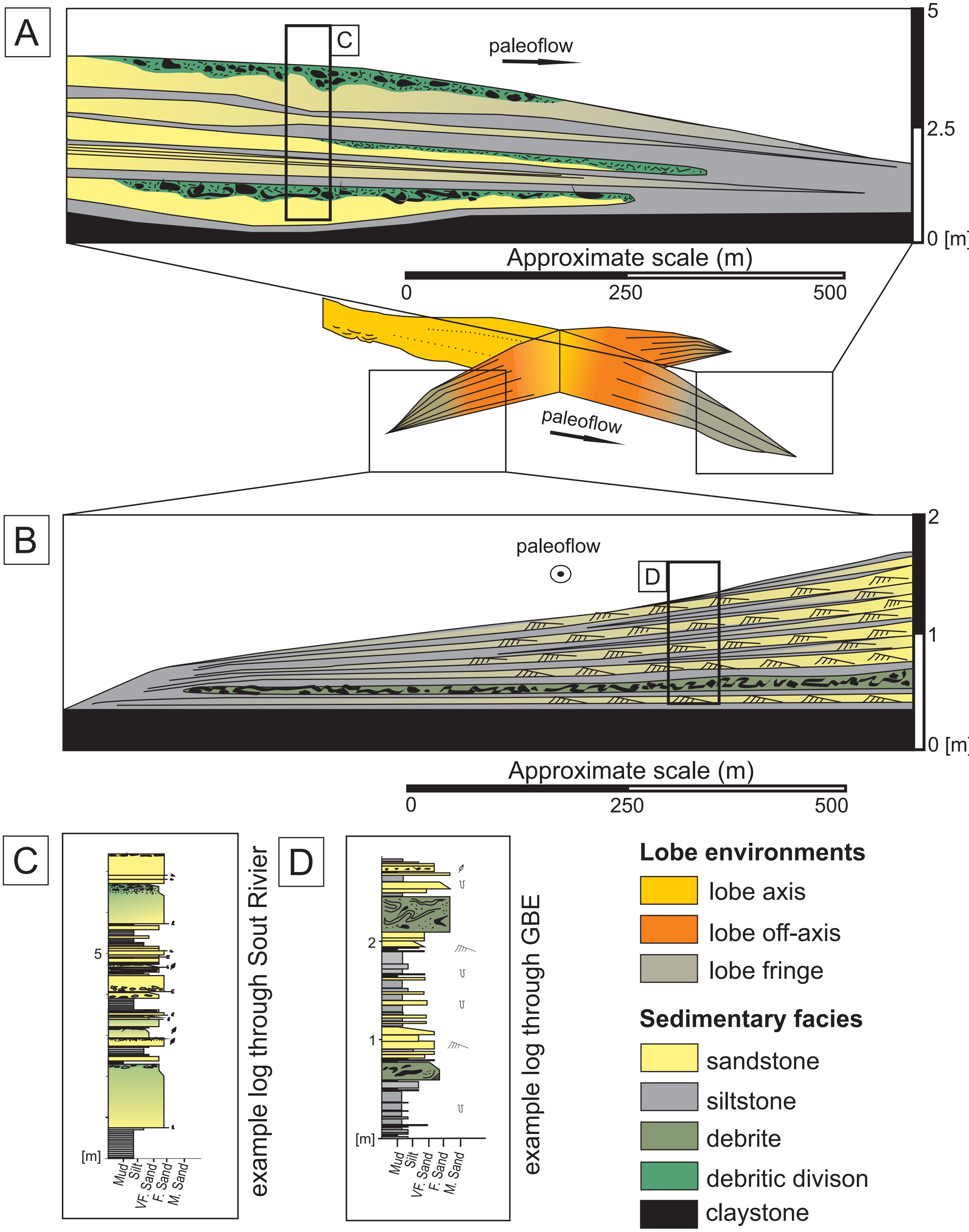

A
C
paleoflow
5
2.5
0 [m]
Approximate scale (m)
0
250
500
paleoflow
B
paleoflow
D
2
1
0 [m]
Approximate scale (m)
0
250
500
C
5
[m]
Mud
Silt
VF. Sand
F. Sand
M. Sand
example log through Sout Rivier
D
2
1
[m]
Mud
Silt
VF. Sand
F. Sand
M. Sand
example log through GBE
Lobe environments
lobe axis
lobe off-axis
lobe fringe
Sedimentary facies
sandstone
siltstone
debrite
debritic divison
claystone

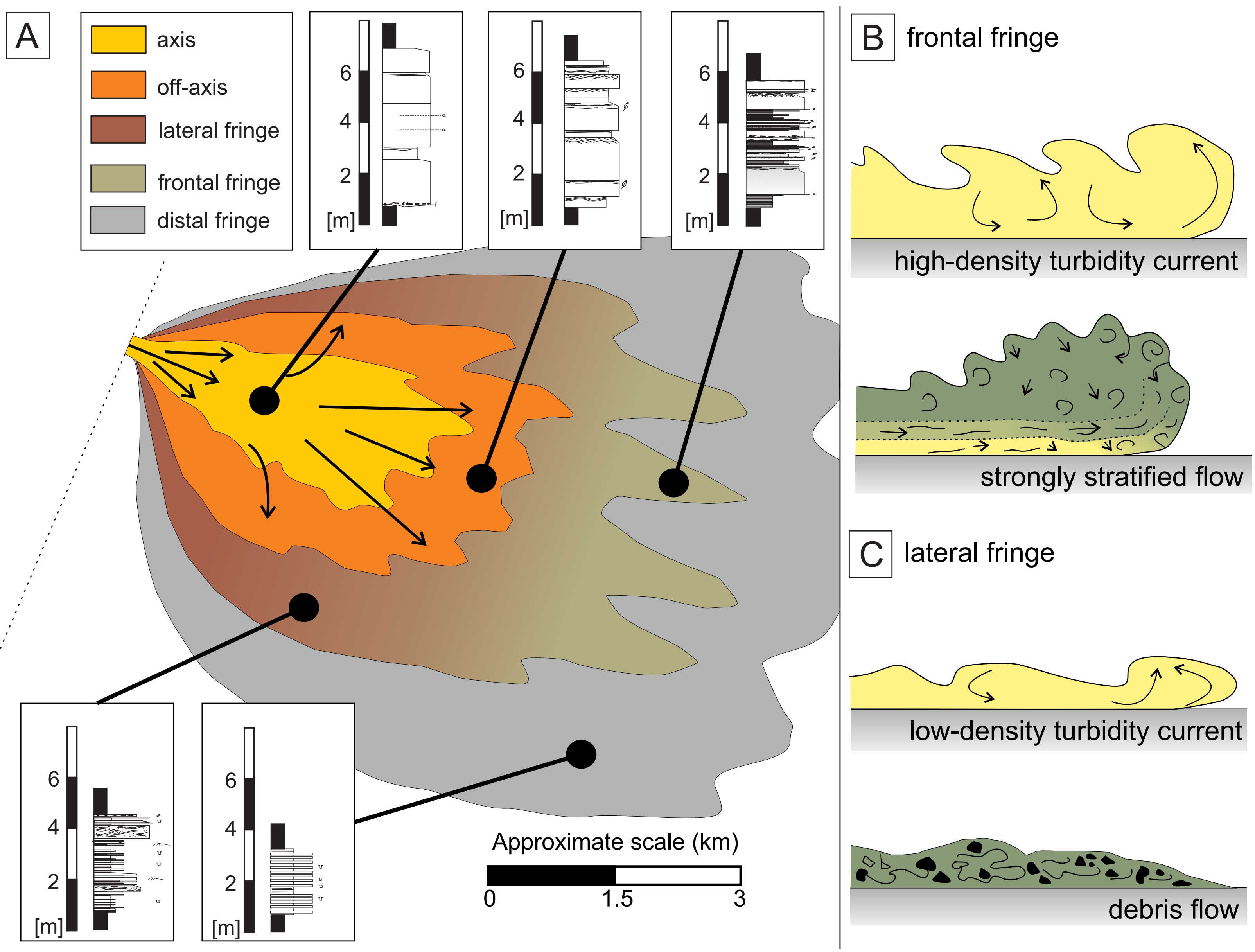

A
axis
off-axis
lateral fringe
frontal fringe
distal fringe
6
4
2
[m]
Approximate scale (km)
0
1.5
3
B
frontal fringe
high-density turbidity current
strongly stratified flow
C
lateral fringe
low-density turbidity current
debris flow

Table 1: Observed lithofacies in Fan 4, their process interpretation and depositional environment

Lithofacies	Grain size	Thickness range	Description	Process interpretation	Depositional environment
Structureless sandstone (F1)	fs to vfs	0.2-2.0 m	Sharp, erosional or loaded base; flute and tool marks common; form high amalgamation units; dewatering common at the base; up to 5% mudstone chips and carbonaceous material in matrix	Deposited by high-density turbidity currents (Kneller and Branney, 1995) with high aggradation rates (Arnott and Hand, 1989; Leclair and Arnott, 2005; Talling et al., 2012a)	Commonly deposited in lobe axis setting, but also observed in lobe fringe settings
Structured sandstone (F2)	fs to vfs	0.1 to 0.7 m	Planar, current-ripple, low-angle climbing-ripple or wavy laminations; normal grading; bed bases are sharp or loaded; bed tops are sharp and flat or undulating; may contain carbonaceous material at the top	Deposited by low-density turbidity currents. Planar and current-ripple lamination produced by reworking through dilute flows along the bed (Allen, 1982; Southard, 1991; Best and Bridge, 1992). Climbing-ripple lamination forms under bedload transport associated with high aggradation rates (Allen, 1973; Hunter, 1977; Jobe et al., 2012). Wavy or sinusoidal lamination indicates deposition from waning currents with very high rates of suspension fallout (Allen, 1973; Jopling and Walker, 1968; Hunter, 1977)	Deposited in lobe off-axis setting
Banded sandstone (F3)	fs to vfs	0.1 to 1.5 m	Couplets of dark and light bands; Light bands comprise "clean" sandstone; dark bands are mud-rich and can comprise mudstone chips and carbonaceous material; band thickness varies from 0.2 to 1 cm; bands can be continious or discontinuous over the distance of several meters	Deposited by transitional flows. Fluctuations of clay content of near-bed layers result in flows alternating between fully turbulent and more cohesive viscous types, thereby depositing alternating clean and argillaceous sand laminae (Lowe and Guy, 2000; Davis et al., 2009; Haughton et al., 2009)	Observed at the boundary between lobe-axis to off-axis settings
Hybrid beds (F4)	fs to vfs	0.05 to 1.5 m	Consists of two divisions. Lower division: well sorted and "clean" with mudstone chips to the top; Upper division can be: 1) mudstone- and siltstone-clast rich with clean matrix; 2) argillaceous, poorly sorted sandstone with a swirly and patchy fabric comprising mudstone chips and carbonaceous material; or 3) argillaceous, micaceous, poorly sorted, clast-rich sandstone	Deposited from strongly stratified flows (e.g. Kane and Pontén, 2012; Talling, 2013) and from co-genetic turbidity currents (lower division) and cohesive debris flows (upper divisions) (Haughton et al., 2003; Talling et al., 2004; Haughton et al., 2009, Hodgson, 2009). Hybrid beds with an upper clast-rich division are interpreted to be formed as a suspension deposit from a purely turbiditic current (Hodgson, 2009) due to local entrainment of heterolithic material	Deposited in lobe fringe environments
Debrites (F5)	fs to vfs	0.2 to 3 m	Poorly sorted; mud-rich; outsized quartz grains (ufs); variable amount of mudstone chips, siltstone clasts, and carbonaceous material	Deposited by en masse freezing of debris flows (Iverson, 1997; Talling et al., 2012a).	not indicative of any environment
Heterolithic packages (F6)	vfs and silt	0.05 to 0.3 m	Sandstone beds show planar, wavy, current-ripple, and stoss-side-preserved climbing-ripple lamination; . Siltstones are stuctureless to planar laminated; normal grading; sharp bed bases; undulating tops due to preservation of ripple crests	Deposits of distal, sluggish, low-volume flows (cf. Jobe at al., 2012). Ripple lamination form beneath dilute turbulent flows via reworking of the bed under moderate aggradation rates, whereas climbing-ripple lamination forms under high aggradation rates (Allen, 1971; Allen, 1982; Southard, 1991)	Deposited in lobe fringe environments
Siltstone (F7)	fine to coarse silt	0.01 to 0.2 m	Structureless, planar-laminated or current-ripple-laminated (where sandy); bioturbation is common;	Deposited by dilute turbidity currents. Planar lamination is a product of traction (Stow and Piper, 1984; Mutti, 1992; Talling et al., 2012a). Structureless beds are formed by direct suspension fallout (Bouma, 1962)	Deposited in lobe distal fringe environments
Claystone (F8)	clay	0.005 to 0.02 m	Commonly silty; concretions associated with distinctive horizons	Suspension fall-out	Hemipelagic background deposits

Table 2: Geometry and lithofacies criteria of frontal lobe fringes and lateral lobe fringes

Characteristics	Frontal lobe fringe	Lateral lobe fringe
Bed thickness	highly variable; 0.1-1.5 m	0.05-0.2 m
Average grain size/ sand vs silt	25-45% silt	60-80% silt
Outcrop geometries	tabular to lenticular	tabular
pinchout geometries	finger-like with abrupt pinchout	wedge shaped; gradual
Current-ripple lamination?	rare	common
Climbing-ripple lamination?	rare	rare
Multidirectional palaeoflow indicators?	rare	common
Hybrid beds?	common	rare
Climbing bedforms?	rare	rare
Debrites?	rare	rare